



**Calhoun: The NPS Institutional Archive**  
**DSpace Repository**

---

Theses and Dissertations

1. Thesis and Dissertation Collection, all items

---

1987

An AB intio study of dimethyl nitramine.

Cordell, Floyd Richard

---

<http://hdl.handle.net/10945/22587>

---

*Downloaded from NPS Archive: Calhoun*



<http://www.nps.edu/library>

Calhoun is the Naval Postgraduate School's public access digital repository for research materials and institutional publications created by the NPS community. Calhoun is named for Professor of Mathematics Guy K. Calhoun, NPS's first appointed -- and published -- scholarly author.

**Dudley Knox Library / Naval Postgraduate School**  
**411 Dyer Road / 1 University Circle**  
**Monterey, California USA 93943**



DURHAM COUNTY COURTHOUSE  
NORTH CAROLINA 27701  
LITIGATION DIVISION 336-6002





# AN AB INITIO STUDY OF DIMETHYL NITRAMINE

APPROVED:

---



To Sandi, Becca and E-Beth



# AN AB INITIO STUDY OF DIMETHYL NITRAMINE

by

Floyd Richard Cordell, B.S.

THESIS

Presented to the Faculty of the Graduate School of

The University of Texas at Austin

in Partial Fulfillment

of the Requirements

for the Degree of

Master of Arts

THE UNIVERSITY OF TEXAS AT AUSTIN

August 1987

T233167



# ACKNOWLEDGMENTS

In the parlance of Naval Aviation, "this is the fun part" of the paper. Thanking all the people who make you look great is always fun, but first some official business. This work has been supported by the United States Navy's Civilian Institution Post-graduate Education Program and the Robert A. Welch Foundation.

I must thank the people that made it possible for me to attend the University of Texas. Dr. Marye Anne Fox, Dr. Stephen Webber and Vickie Masters struck a true blow for freedom in the Spring of 1985. In less than three months, they cut through the Naval Sea Systems Command bureaucracy and had the University placed on the "Approved" list of civilian institutions. Vickie Masters receives another set of kudos for getting my orders changed for the third or fourth time and sparing me from being sent to Kansas.

Hugh Rand has been forced to endure cruel and unusual punishment throughout my thesis writing. He was the first person to read the twisted and muddled thoughts that eventually became this thesis. Without his efforts, I would still be working on the introduction.

Dr. Robert Wyatt and Dr. Richard Friesner kindly agreed to sit as committee members for this thesis. I greatly appreciate their efforts to teach me the vagaries of statistical and quantum mechanics.

Connie Kanetzky is a wonderful secretary and friend. Perhaps the most important effort she has undertaken in the last two years, is the pursuit of the perfect donut. Her efforts made the weekly



AIP seminar survivable.

Dr. James E. Boggs has been an important influence in my life since my first dark days as an undergraduate. He has always been able to point me in the right direction when I get lost. I can not adequately express my thanks for all that Dr. Boggs has done for and meant to me.

My parents had some small part in getting me on this earth. More importantly, they gave me a strong desire to succeed and taught me the value of taking pride in one's work.

Finally, I thank my wife, Sandi, and my daughters, Rebecca and Elizabeth, for their patience and understanding over the last two years. I am sure they would have gladly sent me back to the "boat" to escape my grumpiness when the computer just would not admit it was wrong and I was right.



# ABSTRACT

The structure of dimethyl nitramine is optimized with the 4-21NO\* and 6-31G\* basis sets. The most stable configuration is non-planar in agreement with the low temperature x-ray diffraction structure, but in disagreement with the electron diffraction structure.

One dimensional potential surfaces are calculated for the NO<sub>2</sub> inversion, N-N torsion and methyl inversion internal coordinates. The NO<sub>2</sub> inversion is described the the equation:

$V(x) = .00376 + 0.00418x + .01737x^2$ ; V in kcal/mole and x in degrees.

The N-N torsion is dominated by the twofold term. The 6-31G\* basis set determines the rotational barrier height to be 11.35 kcal/mole and the potential surface is described by the equation:

$$V(x) = 5.692(1 - \cos(2x)) + .332(1 - \cos(4x));$$

V in kcal/mole and x in degrees.

Methyl group inversion is a very low energy motion. Changing the coordinate from the planar position to 40° out-of-plane requires only 400 cal/mole. Methyl group inversion is described by the equation:

$$V(x) = 0.405 - 0.9092E-03x^2 + 0.4518E-06x^4 + 0.6643E-10x^6;$$

V in kcal/mole and x in degrees.

The methyl group inversion ground vibrational state is below the



inversion barrier, while all of the excited states are above the barrier.

The 4-21NO\* basis set is shown to overestimate the non-planar nitrogen of nitrogen, while the 6-31G\* basis set is shown to underestimate the non-planar nature of nitrogen. The 4-21NO\* basis set calculates inversion barriers that are too high and rotational barriers that are too low compared to barriers calculated with 6-31G\* basis set.



# TABLE OF CONTENTS

|   |      |
|---|------|
| Acknowledgments .....                   | iv   |
| Abstract .....                          | vi   |
| Table of Contents.....                  | viii |
| List of Tables.....                     | ix   |
| Chapter One .....                       | 1    |
| Introduction .....                      | 1    |
| Chapter Two .....                       | 5    |
| Methods.....                            | 5    |
| Level of Theory and Basis Set .....     | 5    |
| Calculation of Potential Surfaces ..... | 23   |
| Chapter Three .....                     | 25   |
| Dimethyl Nitramine .....                | 25   |
| Review of Previous Work.....            | 26   |
| Dimethyl Nitramine Geometry .....       | 31   |
| Coordinate 17.....                      | 34   |
| Coordinate 14 .....                     | 49   |
| Coordinate 28.....                      | 62   |
| Concluding Remarks.....                 | 77   |
| Chapter Four.....                       | 79   |
| Conclusion .....                        | 79   |
| Appendix .....                          | 82   |
| Bibliography.....                       | 97   |
| Vita .....                              | 100  |



# LIST OF TABLES

|  |    |
|--|----|
| Table 2-1 Nitromethane Geometries .....                                      | 12 |
| Table 2-2 Formamide Geometries.....  | 15 |
| Table 2-3 Formamide Geometry Differences .....                               | 21 |
| Table 2-4 Formamide Calculated Barrier Heights.....                          | 22 |
| Table 3-1 Dimethyl Nitramine Geometries .....                                | 32 |
| Table 3-2 Coordinate 17 .....  | 36 |
| Table 3-3 Gross Atomic Populations at the 6-31G* Optimized<br>Geometry ..... | 47 |
| Table 3-4 Coordinate 14 .....  | 51 |
| Table 3-5 Coordinate 28 .....  | 65 |



# CHAPTER ONE

## Introduction

Theoretical chemistry is rapidly evolving into a powerful predictive tool based on recent improvements in computational methods and computers. Pulay's introduction of the gradient method [1] reduced the time required to calculate an optimum geometry by an order of magnitude and provided the first efficient method for calculating theoretical force fields. More recently, improved integral evaluation [2], SCF convergence [3] and analytical force constant calculation [4] algorithms have further reduced the CPU time required to study a given molecule. Coupling efficient algorithms with supercomputers gives the chemist unprecedented power for the theoretical investigation of chemically interesting systems. Pople's recent review of *ab initio* and correlation methods [5] clearly shows that single determinant SCF calculations are very successful in predicting a wide variety of experimental data. The theoretical results complement and in many instances extend experimental data. More importantly theoretical results are generally obtained faster and at significantly lower cost than corresponding experimental results. Theoretical calculations are particularly useful in the study of subtle structure differences, potential surfaces, molecular force fields and fundamental vibration frequencies.

The primary obstacle to determining an experimental



structure is finding enough independent data to uniquely define the structure. If the required data can not be determined, the experimentalist must impose arbitrary and artificial constraints which limit the accuracy and validity of the structure. All experimental methods are further hampered by vibrational averaging which affects each method differently making it difficult to accurately compare or combine experimental results.

Ab initio calculations can help remedy the above problems. Theoretical structure determination is simply the minimization of a molecule's total energy with respect to changes of the internal coordinates. The optimized structure has a known dependence on the basis set that is reasonably constant from molecule to molecule [6,7]. As a result, structural differences in a single molecule or over a series of related molecules are usually calculated more accurately than they can be determined experimentally. Schafer [8] and Boggs [9] have reported extremely accurate structures by combining experimental and theoretical data. The structures produced in these studies are more accurate than either the theoretical or experimental techniques could produce alone.

Experimental methods can easily determine the height of a rotational or inversion potential barrier very accurately. Accurate determination of the shape of the potential surface requires a series of difficult measurements. Experimental methods can not determine the



other geometry changes that occur when the internal coordinate defining the potential surface is distorted from its equilibrium position.

Rotation and inversion barriers determined by ab initio calculation generally agree with experiment with an accuracy that is adequate for many practical purposes. Additionally, the calculations may be able to accurately determine subtle features in the potential surface and accurately determine the geometry changes that accompany motion over the surface. The theoretical structures are determined without any assumptions regarding the motion over the surface.

In this thesis the results of calculations on dimethyl nitramine,  $(\text{CH}_3)_2\text{NNO}_2$ , are presented. The interest in this compound stems from the United States Navy's Energetic Materials Research Program. The theoretical methods used in this work are presented in Chapter 2. All of the calculations were completed on the University of Texas Center for High Performance Computing Cray-XMP.

A recent study by Gilardi and coworkers [10] finds the nitramine ( $\text{NNO}_2$ ) structure varies widely over a series of related molecules and the results suggest a low inversion barrier. Dimethyl nitramine is studied as a model system for the  $\text{NNO}_2$  group. Chapter 3 presents the dimethyl nitramine results including the optimized geometry and potential surfaces for the N-N torsional, methyl



inversion and NO<sub>2</sub> wagging motions. Chapter 4 presents conclusions and suggestions for future studies.



# CHAPTER TWO

## METHODS

Proper selection of the basis set and level of theory are important first steps in any ab initio calculation. A compromise between the computational cost and the desired accuracy must be reached. In this chapter, I will discuss the methods used in this study. The level of theory and basis set are presented first, followed by a short discussion of the calculation of potential surfaces.

### Level of Theory and Basis Set

Calculation of the exact molecular wavefunction is the ultimate goal of quantum chemistry. Unfortunately, this requires expansion of the wavefunction in an infinitely large basis set and inclusion of an infinite number of configurations, clearly an unreachable goal. In practice one truncates the basis set to a reasonable size and limits the treatment of electron correlation, thereby defining a theoretical model [5]. Proper selection of a model is important, but even more so is recognizing and understanding the limitations imposed by a given model.

Figure 2-1, presented previously [7], provides the basis for choosing a theoretical model. The vertical axis represents the error in some arbitrary structural parameter. The horizontal axis represents



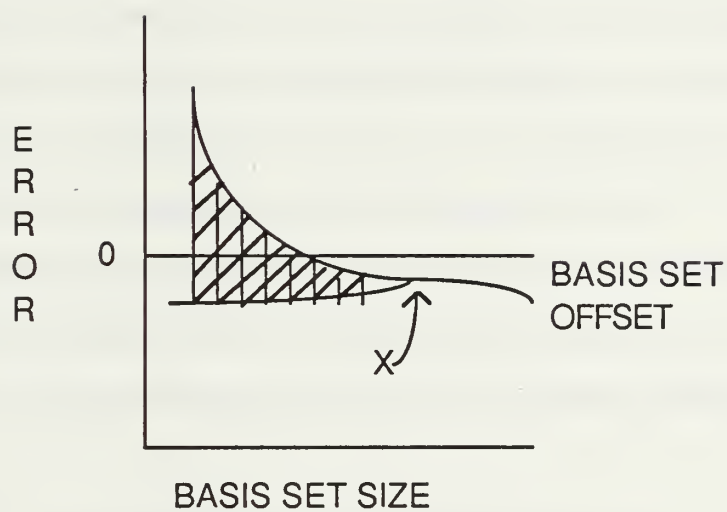
basis set size, increasing to the right. The crosshatched area in Fig. 2-1 represents the scatter of the absolute error, called the relative error, in computation of the same parameter over a series of molecules. At some point (X) the relative error converges to zero, but some absolute error generally remains. The molecular parameter under study determines the basis set size required to converge the relative error. Truncation of the basis set and neglect of electron correlation causes the remaining absolute error, often called the basis set offset. The sum of the basis set offset and the calculated value of a parameter equals the absolute value for the parameter.

For large molecules, one usually performs calculations very close to the point X to reduce the computational cost. The increase in CPU time and disk storage space associated with increasing the size of the basis set is proportional to the fourth power of the number of basis functions ( $N^4$ ).

As the number of basis functions increases, the wavefunction approaches the Hartree-Fock limit where only the electron correlation error remains. Correcting a single determinant Hartree-Fock wavefunction for neglect of electron correlation requires a higher level of theory and is very expensive. The most efficient correlation methods are a minimum of 2 to 3 times more expensive than a single determinant calculation with the same basis set. Algorithms for analytical gradient calculation are not available for correlation



FIGURE 2-1





methods more sophisticated than single and double excitations (CISD) or second order perturbation theory (MP2). Geometry optimization for the more sophisticated correlation techniques is, therefore, prohibitively expensive except for very small or very symmetric molecules.

The size of the molecule considered in this study precludes treatment of electron correlation. Test calculations, described later, showed that Unrestricted Hartree Fock (UHF) theory did not give significantly better results than Hartree Fock theory. Unless stated otherwise the calculations in this study were completed at the single determinant level using the gradient program TEXAS [11].

Before discussing the limitations of the theoretical model, convergence criteria for geometry optimization must be set. A geometry is considered optimized when the following conditions are satisfied:

1. All cartesian forces are less than .005 mdyne/angstrom.
2. Stretching and bending internal coordinate forces are less than .005 mdyne/angstrom or radian.
3. Torsional and out-of-plane internal coordinate forces are less than .001 mdyne/radians.
4. The force on torsional and out-of-plane internal coordinates has changed sign.



Conditions 1 through 3 are standard conditions commonly used for determining geometry convergence. Condition 4 is absolutely necessary to ensure convergence of low energy torsional and out-of-plane motions [12]. The above conditions should give bond lengths to  $\pm 0.001 \text{ \AA}$ , bond angles to  $\pm 0.2^\circ$  and torsional or out of plane angles to  $\pm 2.0^\circ$ .

Chemists have defined many basis sets for ab initio calculations ranging from the minimal STO-3G basis set to very extensive triple zeta plus multiple polarization function basis sets. The selection of a basis set for a particular problem depends on the ab initio program used, the accuracy required and how much CPU time is available to solve the problem. The TEXAS program efficiently uses split valence shell basis sets in which the s and p exponents are constrained to be equal. The 4-21NO\*, Pang's 4-21 basis set [6] augmented with d functions on nitrogen and oxygen, and Pople's 6-31G\* [13] basis sets are used in this study. The d functions are defined as a linear combination of displaced p functions as suggested by Pulay [11]. Studies of substituted dimethyl ethers [14], fluoroboric acids [7] and pyrrolidine [15] have shown that polarization functions are necessary for the proper description of nitrogen and oxygen.

The theoretical model is now defined and we can now thoroughly examine its limitations. The first and perhaps most



fundamental limitation is the assumption that the ground state is adequately described by a closed shell single determinant wavefunction. The nitro ( $\text{NO}_2$ ) group, which is of central importance in this study, requires a multideterminant ground state wavefunction [16,17,18,19]. Its multideterminant nature is due to a small energy gap between a pi-type highest occupied molecular orbital and a  $\pi^*$  type lowest unoccupied molecular orbital. The coefficient of the excited determinant varies from 0.2 to 0.4 depending upon the basis set and method used to treat electron correlation [16,17,19]. The multideterminant ground state creates enormous difficulties in the treatment of electron correlation. Traditional correlation methods, based on the assumption that a single determinant is very strongly dominant, converge very slowly preventing accurate estimation of the correlation energy. Accurate determination of the electron correlation for the nitro compounds requires very costly Multireference Determinant Correlation (MRDCI) methods [16,17,19].

The above discussion suggests that the nitro group poses unusual challenges for theoretical chemistry. The usual assumption that a single determinant dominates the ground state is false, but single determinant calculations may still provide accurate relative values if the contribution of the excited determinant is constant from molecule to molecule. Although MRDCI studies of several different R- $\text{NO}_2$  compounds have been reported, the coefficients of the excited



determinants have been published only for nitromethane. The data presently available, therefore, do not permit determining how the contribution of the excited determinant changes from molecule to molecule. Kaufman and coworkers have studied the change in contribution of the excited determinant as a function of the C-N bond length in nitromethane [18]. They find the contribution is almost constant near the equilibrium geometry, but changes significantly as the C-N bond dissociates. In this study, the primary interest is in structural changes near the equilibrium geometry. Based on the above discussion the following assumptions are used:

- a) The contribution of the excited state determinant is constant.
- b) Geometry correction factors and force constant scale factors correct for the effects of the excited determinant.
- c) Relative values are computed accurately.

A recent study suggests Unrestricted Hartree-Fock theory provides a better description of molecules similar to  $\text{HNO}_2$  than Restricted Hartree Fock theory [20]. Test calculations using Gaussian 82 [21] were completed for nitromethane and azamethine ylide,  $(\text{CH}_2)\text{NH}$  [22]. With the 6-31G\* basis set the nitromethane UHF energy is about 5 kcal/mole lower than the RHF energy. The UHF NO bond length agrees with experiment better than the RHF NO bond length, see Table 2-1, but the RHF CN bond length and ONO angle



TABLE 2-1  
NITROMETHANE GEOMETRIES<sup>a</sup>

|                               | <u>RHF</u> | <u>RHF/MP2</u> | <u>UHF</u> | <u>EXP<sup>b</sup></u> |
|-------------------------------|------------|----------------|------------|------------------------|
| C-N                           | 1.479      | 1.485          | 1.470      | 1.489                  |
| N-O                           | 1.192      | 1.240          | 1.214      | 1.224                  |
| C-H <sub>p</sub> <sup>c</sup> | 1.081      | 1.090          | 1.081      |                        |
| C-H <sub>s</sub> <sup>d</sup> | 1.076      | 1.087          | 1.077      |                        |
| <CNO                          | 117.1      | 117.1          | 118.1      | 117.3                  |
| <ONO                          | 125.8      | 125.8          | 123.8      | 125.4                  |
| <H <sub>p</sub> CN            | 106.8      | 107.3          | 108.2      | 107.2 <sup>e</sup>     |
| <H <sub>s</sub> CN            | 107.8      | 107.7          | 108.1      | 107.2 <sup>e</sup>     |

a. Calculations completed with the Gaussian 82 program and the 6-31G\* basis set.

b. A. P. Cox and S. Waring, J. Chem. Soc. Perkin Trans. 1060 (2) 1972.

c. H<sub>p</sub> is the hydrogen perpendicular to the CNO<sub>2</sub> plane.

d. H<sub>s</sub> is one of the symmetric hydrogens.

e. Average value.



agree with experiment better than the corresponding UHF values.

Dobbs extended his azamethine ylide calculations [22] to include a frequency analysis and electron correlation at the MP2 level. The RHF frequency analysis corresponds to the ground state with all real frequencies while the UHF frequency analysis for the same basis configuration corresponds to a transition state with multiple imaginary frequencies. Further UHF calculations were not conducted because the UHF theory fails to determine geometries superior to RHF theory and fails to determine reasonable vibrational frequencies.

We now examine 4-21NO\* and 6-31G\* basis set effects. Previous experience shows that the calculated equilibrium bond lengths are generally shorter than experiment and calculated bond angles generally agree with experiment. Formamide is a small but complex molecule that provides the basis for an accurate assessment of basis set effects around nitrogen.

Two previous studies of formamide provide the background for the current study. Niu and Boggs studied the effect of increasing basis set size on the formamide geometry with emphasis on the N inversion motion [12]. Krauss and coworkers have studied basis set, electron correlation and geometry optimization effects on the formamide rotation barrier [23]. Reference 12 shows that formamide is a severe test of any basis set due to its very slightly non-planar



geometry.

Krauss and coworkers incorrectly assume the equilibrium structure of formamide [23] is planar and compound their error by believing this assumption does not have a significant effect on the optimized geometry or the height of the rotation barrier. Table 2-2 summarizes the geometries of several different formamide calculations. Comparing the planar 4-21NO\* structure (pg. 17) with the optimized 4-21NO\* structure (pg. 16) shows that small changes in the pyramidal nature of nitrogen can significantly affect other parts of the molecule. The planar C-N bond length is 0.006 Å shorter than optimized bond length. The 4-21NO\* optimized structure is 0.6 kcal/mole more stable than the planar structure. The rotation barriers determined by Krauss et. al. describe the motion from the inversion transition state to the rotational transition state and, therefore, underestimate the true rotation barrier.

Krauss et. al. treat electron correlation using the ACCD and CISD methods at the DZ+D geometry without further geometry optimization. The equilibrium and rotational transition geometries of formamide were calculated in this work using the 6-311G\*\* basis set [24] including electron correlation at the MP2 level. These calculations extend the earlier studies and provide an accurate reference point for examining 4-21NO\* and 6-31G\* basis set effects. Table 2-2 shows that the 4-21NO\* basis set overestimates the non-



TABLE 2-2FORMAMIDE GEOMETRIES<sup>a</sup>

|                               | <u>DZ R<sub>e</sub><sup>b</sup></u> | <u>DZ TS<sup>b</sup></u> | <u>DZ+D R<sub>e</sub><sup>b</sup></u> | <u>DZ+D TS<sup>b</sup></u> |
|-------------------------------|-------------------------------------|--------------------------|---------------------------------------|----------------------------|
| C-O                           | 1.234                               | 1.223                    | 1.206                                 | 1.197                      |
| C-N                           | 1.370                               | 1.435                    | 1.364                                 | 1.440                      |
| C-H                           | 1.087                               | 1.085                    | 1.096                                 | 1.093                      |
| N-H <sub>C</sub> <sup>c</sup> | 0.998                               | 1.003                    | 1.001                                 | 1.010                      |
| N-H <sub>t</sub> <sup>c</sup> | 0.996                               | 1.003                    | 0.998                                 | 1.010                      |
| <NCO                          | 124.3                               | 124.3                    | 124.7                                 | 124.9                      |
| <OCH                          | 121.6                               | 120.5                    | 122.4                                 | 121.4                      |
| <CNH <sub>C</sub>             | 119.3                               | 115.5                    | 119.0                                 | 107.8                      |
| <CNH <sub>t</sub>             | 121.4                               | 115.5                    | 121.5                                 | 107.8                      |
| <OCNH <sub>C</sub>            | 0.0                                 | 67.7                     | 0.0                                   | 56.7                       |



TABLE 2-2 (CONTINUED)

## FORMAMIDE GEOMETRIES

|                               | DZ+D(N) <sup>b</sup> | DZ+D(N) <sup>b</sup> | 4-21NO* <sup>d</sup> | 4-21NO* <sup>d</sup> |
|-------------------------------|----------------------|----------------------|----------------------|----------------------|
|                               | <u>R<sub>e</sub></u> | <u>TS</u>            | <u>R<sub>e</sub></u> | <u>TS</u>            |
| C-O                           | 1.235                | 1.218                | 1.195                | 1.189                |
| C-N                           | 1.365                | 1.437                | 1.373                | 1.446                |
| C-H                           | 1.088                | 1.092                | 1.091                | 1.087                |
| N-H <sub>C</sub> <sup>c</sup> | 1.002                | 1.009                | 1.005                | 1.016                |
| N-H <sub>t</sub> <sup>c</sup> | 0.999                | 1.009                | 1.003                | 1.016                |
| <NCO                          | 124.3                | 122.6                | 125.3                | 125.6                |
| <OCH                          | 121.5                | 119.7                | 122.8                | 122.2                |
| <CNH <sub>C</sub>             | 118.9                | 108.6                | 114.4                | 106.4                |
| <CNH <sub>t</sub>             | 120.9                | 108.6                | 116.4                | 106.4                |
| <OCNH <sub>C</sub>            | 0.0                  | 57.7                 | 16.4                 | 55.1                 |



TABLE 2-2 (CONTINUED)

## FORMAMIDE GEOMETRIES

|                    | 4-21NO*       | 6-31G*d              | 6-31G*d   | 6-311G****e          |
|--------------------|---------------|----------------------|-----------|----------------------|
|                    | <u>PLANAR</u> | <u>R<sub>e</sub></u> | <u>TS</u> | <u>R<sub>e</sub></u> |
| C-O                | 1.198         | 1.193                | 1.183     | 1.186                |
| C-N                | 1.367         | 1.349                | 1.427     | 1.348                |
| C-H                | 1.091         | 1.091                | 1.087     | 1.094                |
| N-H <sub>c</sub>   | 1.001         | 0.996                | 1.006     | 0.994                |
| N-H <sub>t</sub>   | 0.998         | 0.993                | 1.006     | 0.991                |
| <NCO               | 125.5         | 124.9                | 125.1     | 124.9                |
| <OCH               | 122.8         | 122.4                | 121.5     | 122.3                |
| <CNH <sub>c</sub>  | 119.1         | 119.3                | 108.5     | 118.8                |
| <CNH <sub>t</sub>  | 121.4         | 121.7                | 108.5     | 120.7                |
| <OCNH <sub>c</sub> | 0.0           | 0.0                  | 57.0      | 6.5                  |



TABLE 2-2 (CONTINUED)  
FORMAMIDE GEOMETRIES

|                    | MP2 <sup>f</sup>     | MP2 <sup>f</sup> | EXP <sup>g</sup>     | EXP <sup>h</sup>     |
|--------------------|----------------------|------------------|----------------------|----------------------|
|                    | <u>R<sub>e</sub></u> | <u>IS</u>        | <u>R<sub>e</sub></u> | <u>R<sub>e</sub></u> |
| C-O                | 1.213                | 1.206            | 1.193                | 1.219                |
| C-N                | 1.367                | 1.443            | 1.376                | 1.352                |
| C-H                | 1.106                | 1.101            | 1.102                | 1.098                |
| N-H <sub>C</sub>   | 1.008                | 1.018            | 1.014                | 1.002                |
| N-H <sub>t</sub>   | 1.005                | 1.018            | 1.002                | 1.002                |
| <NCO               | 125.0                | 125.5            | 123.8                | 124.7                |
| <OCH               | 123.2                | 121.8            | 123.0                | 122.5                |
| <CNH <sub>C</sub>  | 117.2                | 106.6            | 117.1                | 118.5                |
| <CNH <sub>t</sub>  | 119.5                | 106.6            |                      | 120.0                |
| <OCNH <sub>C</sub> | 11.5                 | 55.3             | 7.0                  | 0.0                  |

- a. Bond lengths in angstroms.
- b. Ref. 23. Equilibrium structure constrained to be planar.
- c. H<sub>C</sub> is cis to oxygen and H<sub>t</sub> is trans to oxygen in the r<sub>e</sub> structure.
- d. This work.
- e. Ref. 23.
- f. This work. MP2 geometry optimization with the 6-311g\*\* basis set.



- g. C. C. Costain and J. M. Dowling, J. Chem. Phys. 32 (1960) 158.
- h. E. Hirota, R. Sugisake, C. J. Nielsen and O. Sorensen, J. Mol. Spectrosc., 49 (1974) 251.



planarity of nitrogen, agreeing with earlier studies [12,25]. The optimized 6-31G\* geometry is surprisingly planar, indicating this basis set tends to underestimate the non-planarity of nitrogen. Adding p functions to the hydrogen basis set, forming the 6-31G\*\* basis, gives a very slightly non-planar geometry, the OCNH<sub>C</sub> torsion angle is 3.5°. The MP2 geometry agrees with the experimental structures to within experimental uncertainty and is slightly more non-planar than the 6-311G\*\*\*\* geometry. Table 2-3 summarizes the equilibrium-transition state geometry differences. The results from various basis sets show excellent agreement with one another except for the 4-21NO\* CNH bond angles and OCNH<sub>C</sub> torsion angle. The 4-21NO\* basis set predicts too small of a change in the CNH angles. The error is due to underestimation of the CNH angles in the 4-21NO\* optimized geometry. The wide range of OCNH<sub>C</sub> torsion angles clearly shows that obtaining an accurate representation of low energy motions around nitrogen is very difficult.

Table 2-4 summarizes several calculated rotation barrier heights. The MP2 optimized barrier is higher than the earlier single point ACCD and CISD barriers calculated at the DZ+D geometry. We cannot critically examine the relative performance of these correlation methods because the experimental gas phase rotational barrier for formamide has not been reported.

The 4-21NO\* basis set underestimates the rotation barrier



TABLE 2-3

## GEOMETRY DIFFERENCES

|                               | 4-21NO* <sup>a</sup>                 | 6-31G* <sup>a</sup>                  | MP2 <sup>a</sup>                     | DZ+D <sup>b</sup>                    |
|-------------------------------|--------------------------------------|--------------------------------------|--------------------------------------|--------------------------------------|
|                               | <u>R<sub>e</sub>-TS</u> <sup>d</sup> | <u>R<sub>e</sub>-TS</u> <sup>d</sup> | <u>R<sub>e</sub>-TS</u> <sup>d</sup> | <u>R<sub>e</sub>-TS</u> <sup>d</sup> |
| C-O                           | 0.006                                | 0.010                                | 0.007                                | 0.009                                |
| C-N                           | -0.073                               | -0.078                               | -0.076                               | -0.076                               |
| C-H                           | 0.004                                | 0.004                                | 0.005                                | 0.003                                |
| N-H <sub>C</sub> <sup>c</sup> | -0.011                               | -0.010                               | -0.010                               | -0.009                               |
| N-H <sub>t</sub>              | -0.013                               | -0.013                               | -0.013                               | -0.012                               |
| <NCO                          | -0.3                                 | -0.2                                 | -0.5                                 | -0.2                                 |
| <OCH                          | 0.6                                  | 0.9                                  | 1.4                                  | 1.0                                  |
| <CNH <sub>C</sub>             | 8.0                                  | 10.8                                 | 10.6                                 | 11.2                                 |
| <CNH <sub>t</sub>             | 10.0                                 | 13.2                                 | 13.0                                 | 13.7                                 |
| <OCNH <sub>C</sub>            | -38.7                                | -57.0                                | -43.8                                | -56.7                                |

a. This work.

b. Ref. 23.

d. R<sub>e</sub>-TS is the optimized value minus the rotational transitional state value for the given parameter.

c. N-H<sub>C</sub> is the N-H bond cis to oxygen. N-H<sub>t</sub> is the N-H bond trans to oxygen.



TABLE 2-4  
CALCULATED BARRIER HEIGHTS

| <u>BASIS SET</u>         | <u>BARRIER</u> |
|--------------------------|----------------|
| DZ/SCF <sup>b</sup>      | 19.1           |
| DZ+D(N)/SCF <sup>b</sup> | 16.2           |
| DZ+D/SCF <sup>b</sup>    | 14.5           |
| TZ+D/ACCD <sup>b</sup>   | 14.3           |
| TZ+D/CISD <sup>b</sup>   | 15.0           |
| 4-21/SCF <sup>c</sup>    | 18.1           |
| 4-21NO*/SCF <sup>d</sup> | 12.0           |
| 6-31G*/SCF <sup>d</sup>  | 15.6           |
| 6-31G**/MP2 <sup>d</sup> | 16.0           |

b. Ref. 23.

c. J. O. Williams, C. Van Alsenoy and L. Schafer, J. Mol. Struct. (THEOCHEM), 76 (1981) 171

d. This work.



while the 6-31G\* basis set provides excellent agreement with the MP2 result. Based on these results, the 4-21NO\* basis set overestimates inversion barrier heights while the 6-31G\* basis underestimates inversion barrier heights. The 6-31G\* basis set is used for the dimethyl nitramine calculations because the interest is in accurate representation of the rotational and inversion potential surfaces. A few calculations were completed using the 4-21NO\* basis set to compare its performance to the 6-31G\* basis set in a more complex molecule.

## CALCULATION OF POTENTIAL SURFACES

The calculation of potential surfaces using theoretical methods is a straightforward task. One could naively assume that the geometry changes linearly from the equilibrium structure to the transition state structure. Chemistry is much more interesting, however, and the structural changes associated with motion over a potential surface are usually nonlinear. The best method for calculating a path along a potential surface is to fix the internal coordinate which defines the path at several different values and then optimize the remaining 3N-7 internal coordinates, assuming a nonlinear molecule. This method ensures that the calculated energies are the best available estimate within the theoretical model. The calculated energies may be



numerically fit to any convenient function. In this study the energies are fit with natural cubic splines and to either a rotational potential function, equation 2-1,

$$V(x) = C_i(1 - \cos(n \cdot x)) \quad (2-1)$$

$C_i$  the maximum amplitude of the given mode

$n$  the order of the axis, i.e. 2-fold, 3-fold, etc

$x$  the value of the internal coordinate

or to a power series expansion, equation 2-2, for deformation modes.

$$V(x) = a + bx + cx^2 + dx^3 + ex^4 + \dots \quad (2-2)$$

Equations (2-1) and (2-2) usually converge very rapidly for well behaved internal motions. The program FUNPLOT, described in Appendix 1, calculates natural cubic spline fits and least squares fits of the input data to any arbitrary function. The program plots the results using the DI-3000 Grafmaker package [26].



## CHAPTER THREE

### Dimethyl Nitramine

The nitramine group,  $\text{NNO}_2$ , is very common in energetic molecules. Several research laboratories are working to synthesize molecules that contain this group and that are more powerful explosives than the commonly used RDX and HMX [10]. To improve on the capabilities of existing explosives, the target molecules contain three or more nitramine groups and are predicted to have densities greater than  $2.0 \text{ gm/cm}^3$ . High density is important in these new compounds to ensure that significant improvements are made in explosive power even though existing warhead casings are used. A simple model is used to predict the density of unknown compounds but it has failed to give accurate results for several molecules. Gilardi and coworkers believe the failure occurs because accurate potential surfaces are not available for the nitramine out-of-plane or torsion motions [10].

The density of nitramine-containing molecules is very sensitive to the conformation of the nitramine group. Gilardi recently completed a survey of structures containing the nitramine group [10]. He found that the angle between the N-N bond and its projection on the CNC plane, angle  $\beta$  in Figure 3-1, varies from  $0^\circ$  to  $39^\circ$  with an average of  $12.2^\circ$ . The wide range of values for  $\beta$  is unexpected and causes difficulties in predicting the density of  $\text{NNO}_2$  containing molecules.



Dimethyl nitramine,  $(\text{CH}_3)_2\text{NNO}_2$ , is a small model system for the nitramine group. Because the molecule is small, we may use a moderately large basis set, 6-31G\*, and should obtain accurate potential surfaces. Figure 3-2 shows the numbering scheme used in this study. Potential surfaces and geometry changes are calculated for the following internal motions of dimethyl nitramine:

- a. N1 moving out of the ONO plane, hereafter called Q17. Figure 3-3 shows this motion.
- b. N2 moving out of the CNC plane, hereafter called Q14. This coordinate corresponds to changing angle  $\beta$  of Figure 3-1.
- c. Torsion of the NN bond, hereafter called Q28.

## REVIEW OF PREVIOUS WORK

The structure of dimethyl nitramine is the subject of one electron diffraction study and several x-ray and neutron diffraction studies. Stolevik and Rademacher determined the gas phase dimethyl nitramine structure by electron diffraction. They concluded the structure is planar [27], although they could not rule out a non-planar structure with the O3NNC5 torsion angle equal to  $14^\circ$ . Stolevik and Rademacher believe the apparent non-planar structure is an artifact of the experiment caused by thermal motion. The planar and non-



Figure 3-1

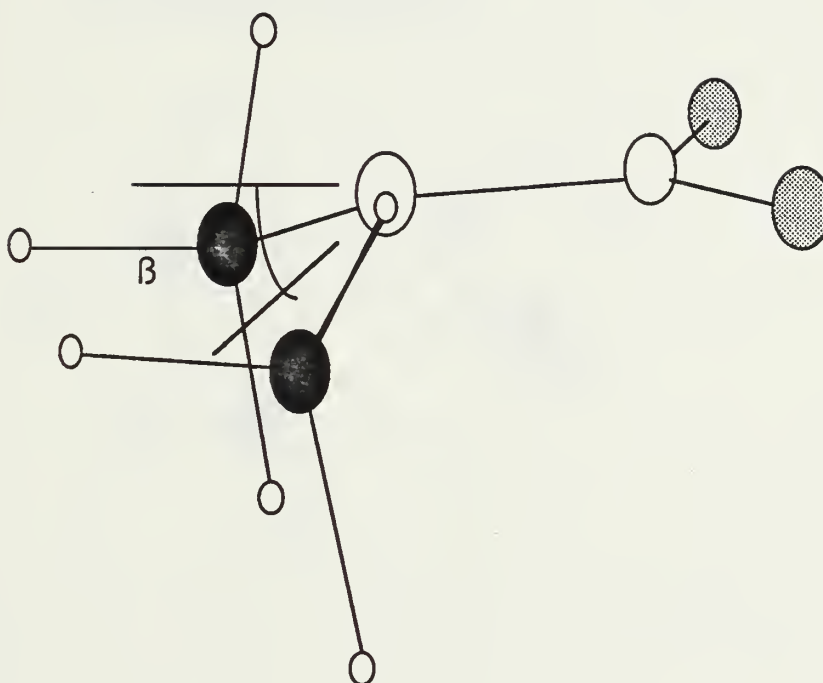
Definition of the Angle  $\beta$ 



FIGURE 3-2

Atom Numbering Scheme  
for Dimethyl Nitramine

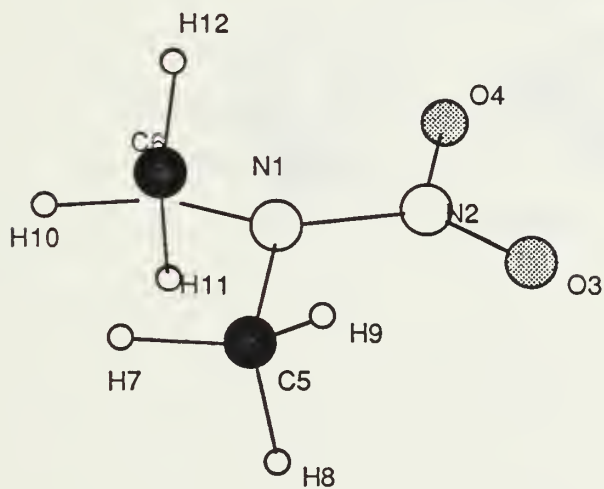
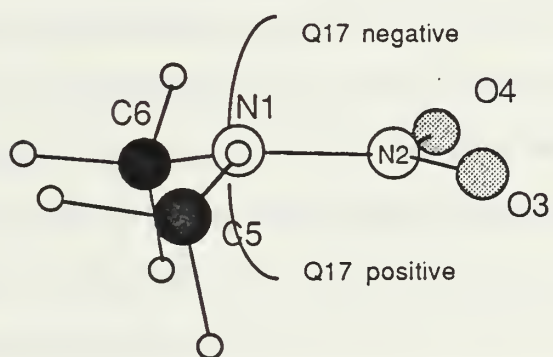




FIGURE 3-3  
DEFINITION OF COORDINATE 17





planar calculated diffraction curves fit the observed curve equally well.

X-ray and neutron diffraction studies show that the dimethyl nitramine geometry changes from a non-planar structure at low temperature to a planar structure at high temperature. Rey-Lafon proposed that a displacive phase transition occurs at 107 K based on changes in the low temperature Raman spectrum [28]. Krebs, Mandt, Cobbledick and Small report a planar structure at 143 K [29] showing that the high temperature geometry is planar. Filhol, Bravic, Rey-Lafon and Thomas confirmed the phase transition with neutron and x-ray diffraction structure determinations [30] at several different temperatures. They determined the low temperature geometry to be non-planar with  $\beta$  equal to  $11.3^\circ$ .

Dimethyl nitramine is the subject of only two previous ab initio studies. Duke optimized the geometry of the  $\text{NNO}_2$  group keeping all other structural parameters fixed and used a minimal basis set [31]. He varied the angle  $\beta$  in his calculations and he found the most stable conformation to be planar. Rezhikova and Shiyapochnikov optimized the geometry and calculated force constants for the  $\text{NNO}_2$  group keeping all other structural parameters fixed, using the STO-3G basis set [32] and assuming the heavy atoms are planar. These studies did not use a large enough basis set to determine accurately if the ground state is planar or non-planar.



## Dimethyl Nitramine Geometry

I optimized the geometry of dimethyl nitramine with the 6-31G\* and 4-21NO\* basis sets. The 4-21NO\* results are compared to the 6-31G\* results to confirm the conclusions presented in Chapter 2. Table 3-1 shows the optimized 4-21NO\* and 6-31G\* geometries and several experimental geometries.

If the 4-21NO\* CN and NO bond lengths are corrected for the basis set offset [33], the electron diffraction planar and corrected 4-21NO\* structures agree to within experimental uncertainty. The electron diffraction non-planar C-N bond length is .007 Å shorter than the corrected 4-21NO\* value. Although this difference is slightly larger than the experimental uncertainty, the agreement between the two structures is still very good.

The electron diffraction CNC and ONO angles are significantly larger than either the ab initio results or the neutron diffraction results and may be in error. The remaining electron diffraction bond angles are within 2° of the ab initio and x-ray diffraction values. Except for the CNC angle, the non-planar electron diffraction bond angles are in better agreement with the ab initio values than are the planar electron diffraction bond angles.



TABLE 3-1<sup>a</sup>

## Dimethyl Nitramine Geometries

|                      | 4-21NO* <sup>b</sup> | 6-31G* <sup>b</sup> | ED <sup>c</sup> | ED(NP) <sup>d</sup> | ND(85 K) <sup>e</sup> |
|----------------------|----------------------|---------------------|-----------------|---------------------|-----------------------|
| N-N                  | 1.372                | 1.343               | 1.3832(26)      | 1.4024(32)          | 1.323(3)              |
| O-N                  | 1.194 <sup>f</sup>   | 1.197               | 1.2250(10)      | 1.2259(8)           | 1.238(5)              |
| C-N                  | 1.470 <sup>f</sup>   | 1.455               | 1.4627(26)      | 1.4536(21)          | 1.459(4)              |
| H7-C5                | 1.079                | 1.080               |                 |                     | 1.09(1)               |
| H8-C5                | 1.075                | 1.077               | 1.1148(52)      | 1.1142(51)          | 1.06(1)               |
| H9-C5                | 1.084                | 1.085               |                 |                     | 1.11(1)               |
| <ONN                 | 116.8                | 117.4               | 114.80(65)      | 115.51(36)          | 118.4(3)              |
| <ONO                 | 126.5                | 125.2               | 130.40(1.30)    | 125.48(66)          | 123.3(3)              |
| <CNN                 | 113.1                | 115.8               | 116.20(28)      | 115.66(19)          | 117.3(2)              |
| <CNC                 | 117.1                | 120.4               | 127.61(55)      | 128.57(37)          | 124.2(3)              |
| <H7-CN               | 107                  | 107.1               |                 |                     | 107.4(5)              |
| <H8-CN               | 109.4                | 110.0               | 101.91(1.93)    | 100.98(1.56)        | 109.2(6)              |
| <H9-CN               | 112.1                | 112                 |                 |                     | 111.5(7)              |
| <H9-C-H8             | 109.4                | 109.1               |                 |                     |                       |
| d(1342) <sup>g</sup> | 2.1                  | 1.2                 | 0.0             | n/a                 |                       |
| d(2651) <sup>g</sup> | 41.3                 | 28.8                | 0.0             | n/a                 | 11.3(3)               |
| t(3215) <sup>h</sup> | -23                  | -16.1               | 0.0             | -12.0               |                       |
| d(4312) <sup>g</sup> | -1.90                | -1.1                | 0.0             | n/a                 |                       |
| E(H) <sup>i</sup>    | -337.041602          | -337.700502         |                 |                     |                       |



- a. Bond lengths in angstroms. Bond angles in degrees.
- b. This work.
- c. Planar geometry from reference 27.
- d. Non-planar geometry from reference 27.
- e. Neutron diffraction 85 K structure from reference 29.
- f. The corrected NO bond length is 1.222 Å and the corrected CN bond length is 1.462 Å.
- g.  $d(ijkl)$  is the angle between the  $il$  vector and the  $jk$  plane.
- h.  $t(ijkl)$  is the angle between the  $ijk$  and  $jkl$  planes.
- i. Total energy in hartrees.



Comparing the ab initio and 85 K neutron diffraction geometries reveals several differences. Because the dimethyl nitramine crystal lattice breaks the  $C_s$  symmetry of the molecule, Table 3-1 shows average solid state values to provide a better comparison to the ab initio and electron diffraction data. The neutron diffraction N-N bond length is shorter and the N-O bond length longer than the ab initio and electron diffraction values. Intermolecular bonding and thermal motion in the crystal may cause the longer N-O bond, but these effects cannot cause the observed shortening of the N-N bond. The most probable cause of the observed N-N bond length is residual disorder in the crystal. Rey-Lafon states that crystal disorder prevented him from obtaining polarized Raman spectra for  $(CD_3)_2NNO_2$  [28].

### Coordinate 17

Internal coordinate 17 (Q17) is the motion of N1 out of the ONO plane, shown in Figure 3-3. We might expect the potential surface describing Q17 to be very anharmonic because motion in the positive direction is primarily affected by CN bonds and the methyl groups while motion in the negative direction is primarily affected by the N1 lone pair. Table 3-2 summarizes the energy and geometry changes as a function of change in Q17. Figure 3-4 is a plot of the potential



energy against change in Q17. The optimum value for Q17 is  $1.2^\circ$ , i.e. N2 is very slightly pyramidal. The calculated potential surface is a true single well.

The Q17 potential surface is almost harmonic over the range investigated in this study. The difference in the potential energy at  $20^\circ$  and  $-20^\circ$  is only 200 cal/mole. Equation 3-1 is the result of a least squares fit to a displaced harmonic oscillator potential function.

$$V(X) = .00376 + 0.00418X + .01737X^2 \quad (3-1)$$

V is in kcal/mole.

X is the displacement of Q17 from the equilibrium position.

The standard deviation of equation 3-1 is 18 cal/mole.

Figure 3-5 shows a plot in the yz plane of the localized orbital, according to Boys criterion [34], that corresponds to the N-N bond. Figure 3-6 shows a similar plot of the N1 lone pair. The center of electron density in Figure 3-5 is slightly below the line joining N1 and N2. Figure 3-6 shows that the electron density of the lone pair shifts toward N2. The implication of these two plots is that the N1 lone pair makes a significant contribution to the N-N bond and that the bond contains some pi type character. The bonding at N1 is, therefore, neither a pure  $sp^2$  hybrid nor a pure  $sp^3$  hybrid. The optimized geometry, in particular the bond angles, shows that the bonding is



TABLE 3-2<sup>a</sup>

Coordinate 17

| Del Q17 <sup>b</sup> | Delta E <sup>c</sup> | N-N   | O-N   | C-N   |
|----------------------|----------------------|-------|-------|-------|
| -20                  | 6.861                | 1.370 | 1.197 | 1.457 |
| -5                   | 0.447                | 1.343 | 1.197 | 1.455 |
| 0                    | 0.000                | 1.343 | 1.197 | 1.455 |
| 5                    | 0.433                | 1.345 | 1.197 | 1.455 |
| 20                   | 7.042                | 1.340 | 1.201 | 1.452 |
| Del Q17              | NNO                  | ONO   | CNN   | CNC   |
| -20                  | 115.3                | 125.3 | 114.7 | 117.0 |
| -5                   | 117.3                | 125.2 | 115.9 | 120.6 |
| 0                    | 117.4                | 125.2 | 115.8 | 120.4 |
| 5                    | 117.2                | 125.2 | 115.8 | 120.1 |
| 20                   | 115.8                | 125.2 | 116.9 | 122.9 |

a. Bond lengths in angstroms. Bond angles in degrees.

b. Change in Q17 from the equilibrium value of 1.2°. Q17 is defined in Figure 3-3.

c. Change in energy in kcal/mole.



FIGURE 3-4  
Q17 POWER SERIES TO  $X^2$

37

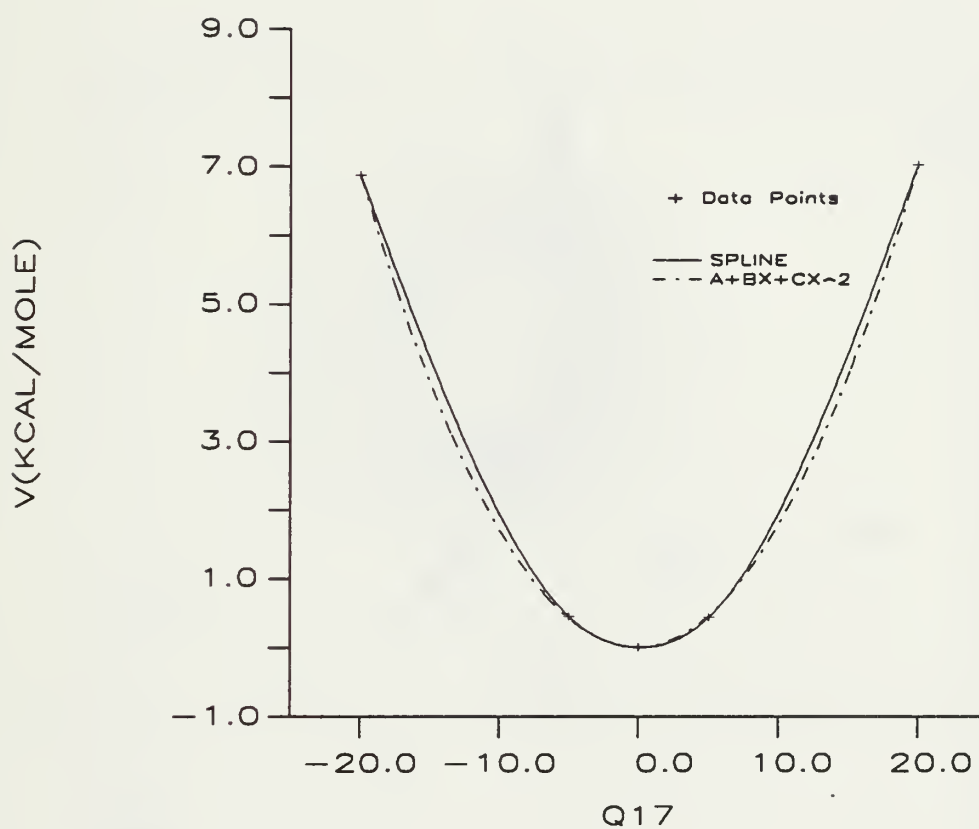




FIGURE 3-5

N-N Bond

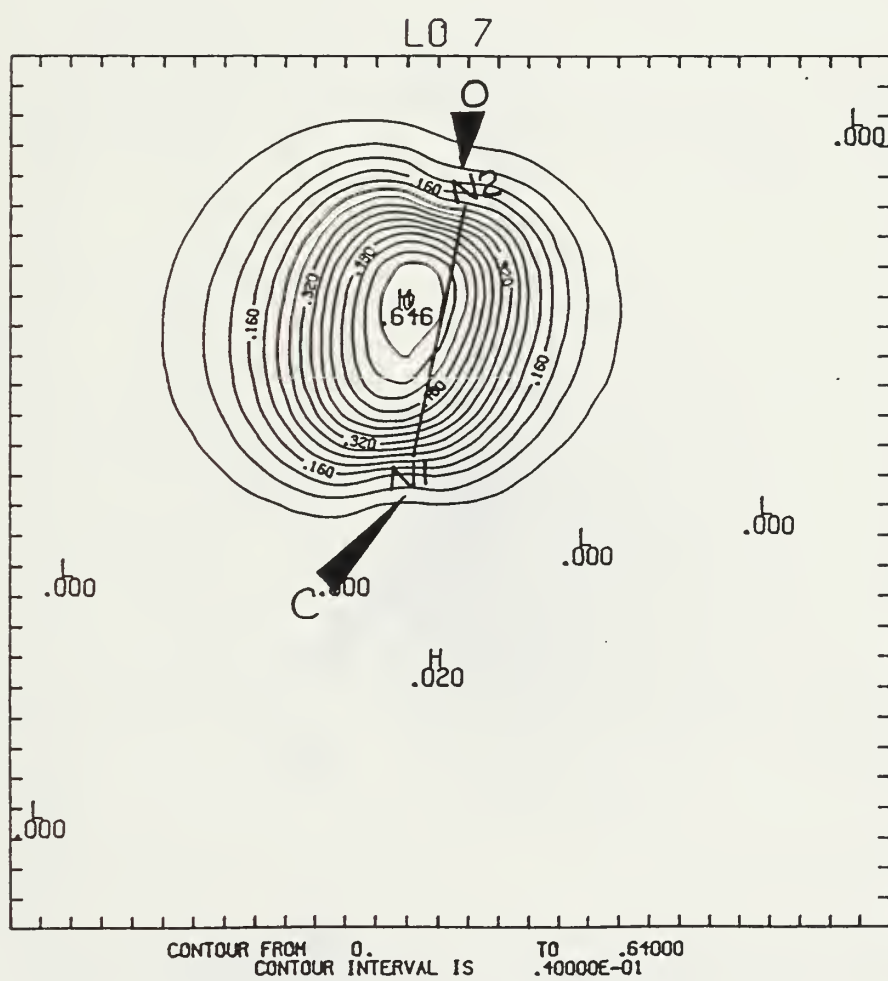




FIGURE 3-6

N1 Lone Pair

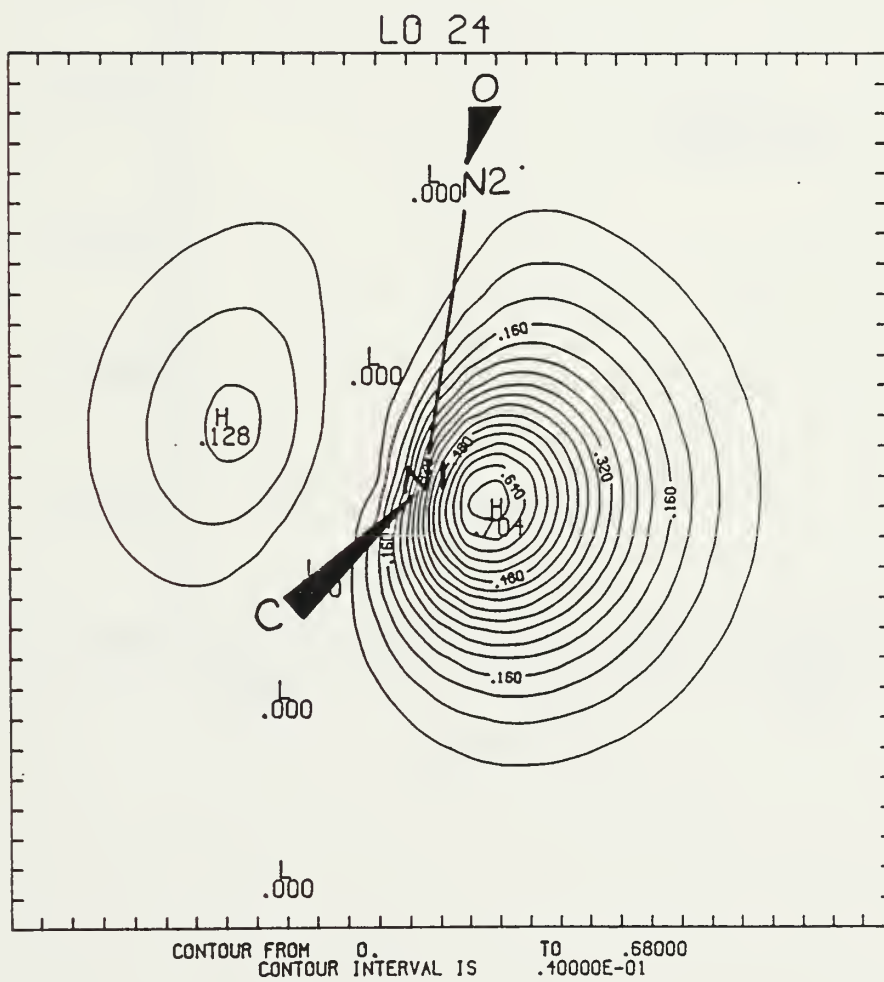




FIGURE 3-7  
Q17 N-O

4C

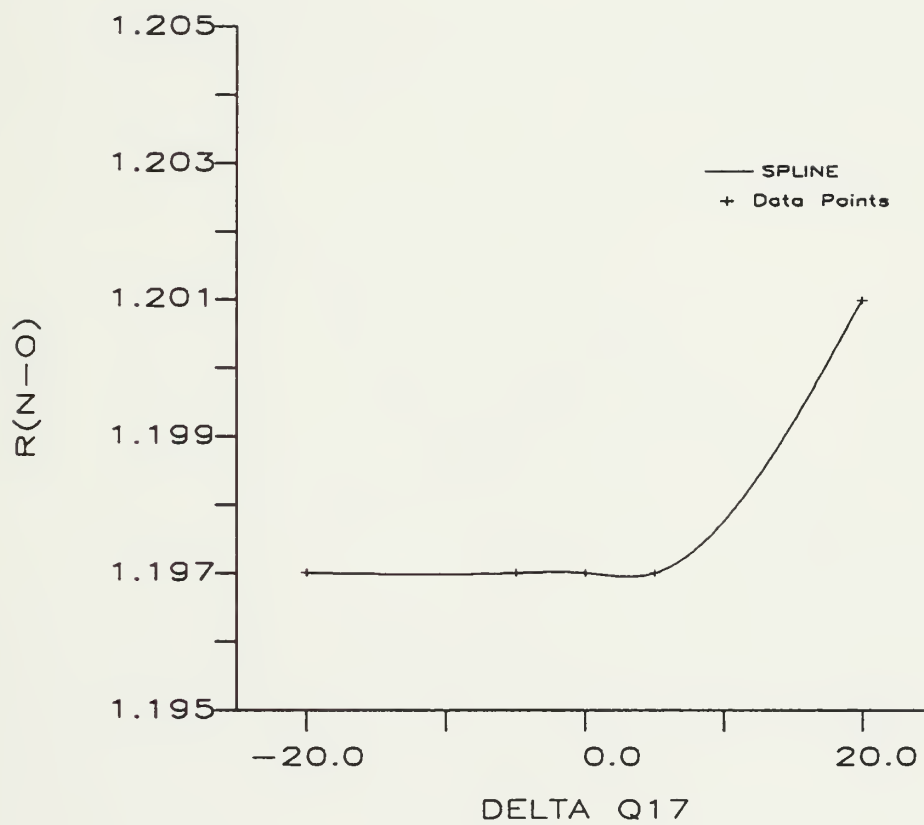




FIGURE 3-8  
Q17 C-N

41

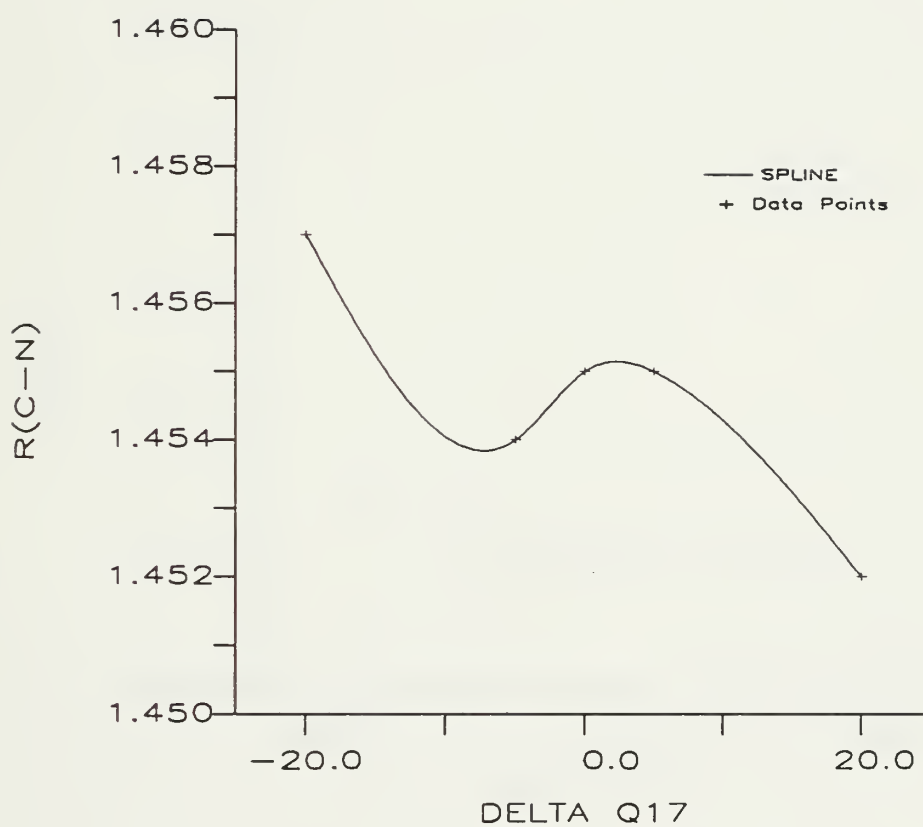




FIGURE 3-9  
Q17 < ONO

42

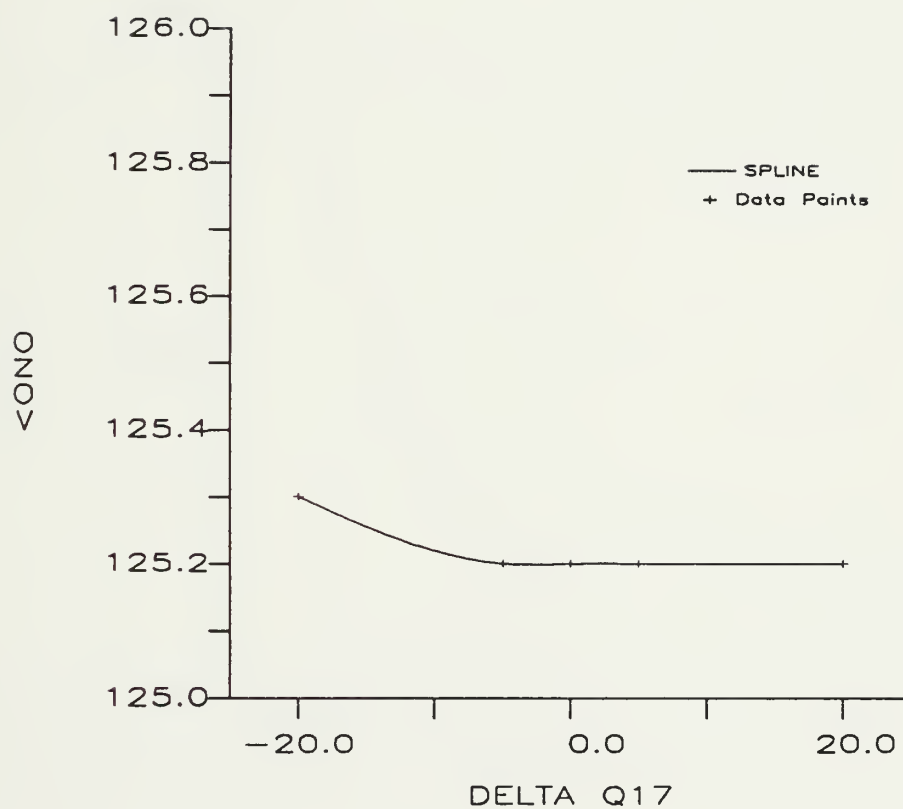




FIGURE 3-10  
Q17 N-N

43

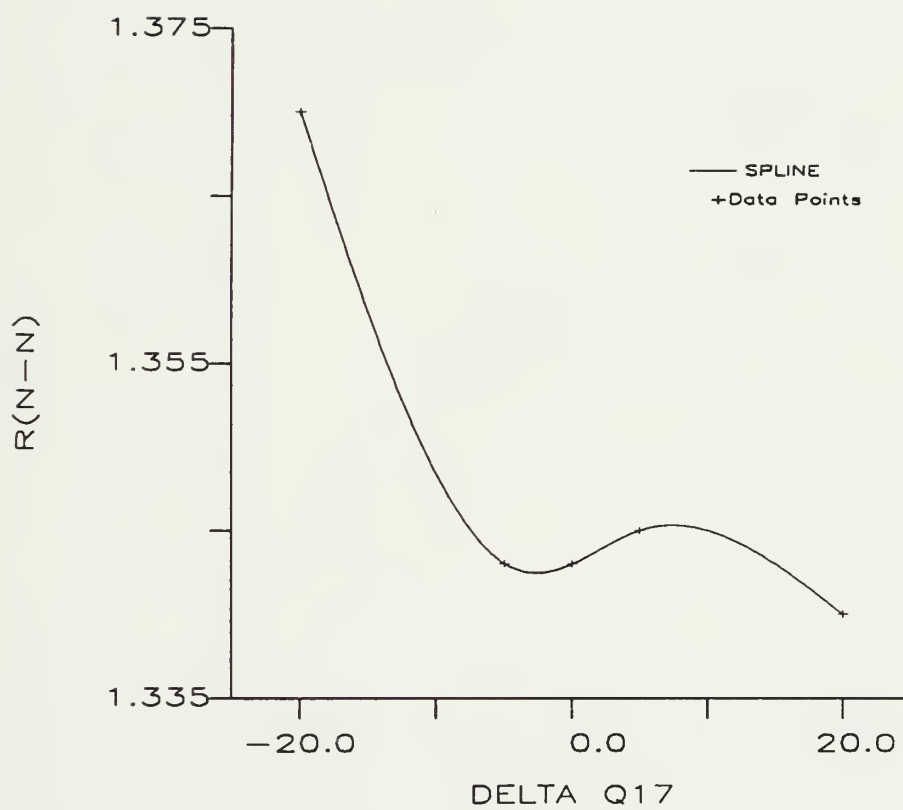




FIGURE 3-11  
Q17 <CNC

44

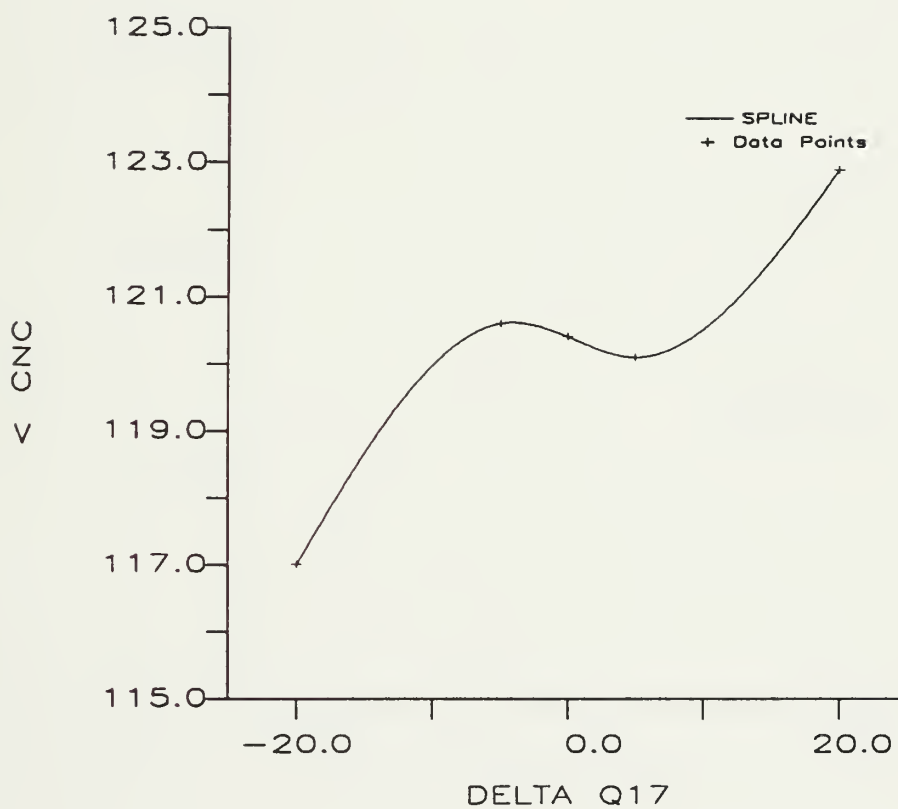




FIGURE 3-12  
Q17 < ONN

45

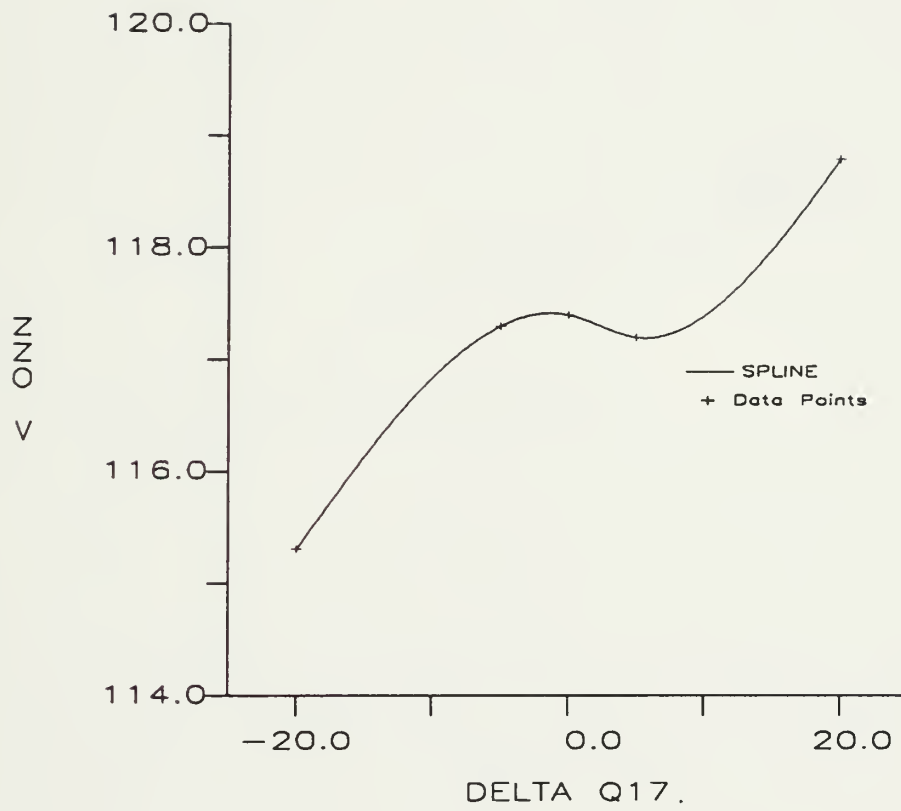




FIGURE 3-13  
Q17 < CNN

46

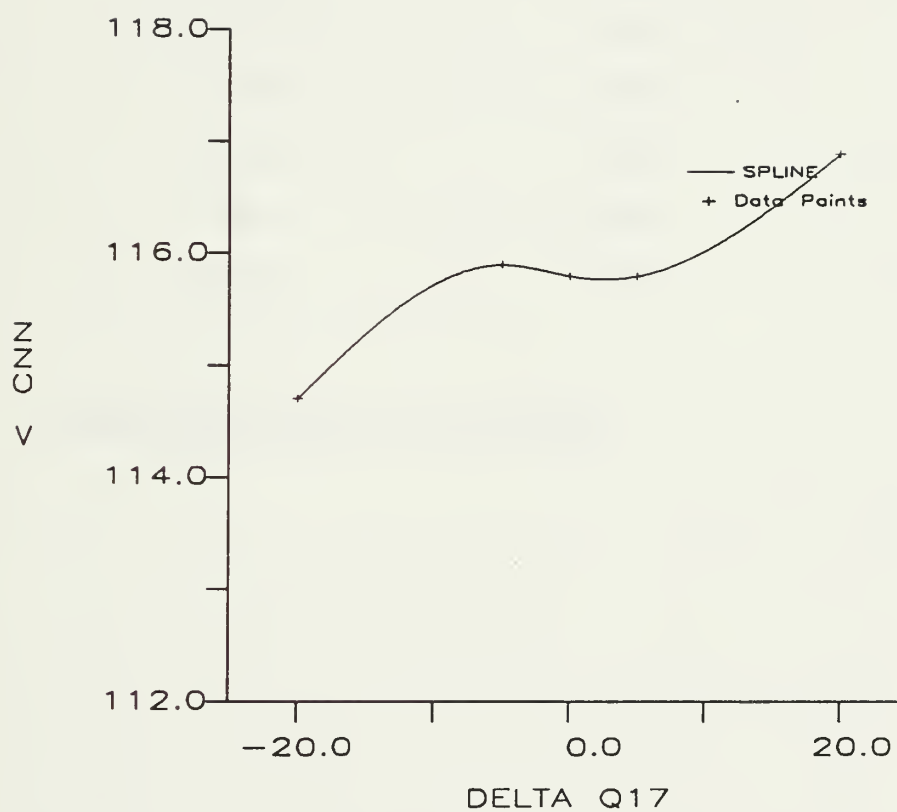




TABLE 3-3<sup>a</sup>

Gross Atomic Populations at the 6-31G\* Optimized Geometry

| Atom | Charge |
|------|--------|
| N1   | -0.45  |
| N2   | 0.88   |
| O    | -0.54  |
| C    | -0.29  |
| H7   | 0.19   |
| H8   | 0.22   |
| H9   | 0.19   |

a. See Figure 3-2 for atom numbering.



more nearly  $sp^2$  than  $sp^3$ .

We now consider geometry changes associated with the Q17 potential surface. Figures 3-7 through 3-13 are plots of various bond lengths and bond angles as a function of change in Q17. Figures 3-7 through 3-9 show that the N-O and C-N bond lengths and the ONO angle do not change significantly. Figure 3-10 shows that the N-N bond shortens for negative displacements and remains almost constant for positive displacements of Q17. Figures 3-11 through 3-13 show that the CNC, ONN and CNN angles change in a similar manner, becoming shorter with negative displacements of Q17 and longer with positive displacements of Q17.

The geometry changes suggest that although the potential surface is almost symmetric, the causes of the energy changes are very different. When Q17 moves in the negative direction, the partial N-N pi bond is broken and the bonding at N1 becomes more like an  $sp^3$  hybrid. When Q17 moves in the positive direction, the N-N bond length does not change. Table 3-3 shows the net atomic charges from a Mulliken Population Analysis [35] for the 6-31G\* optimized geometry. The O, C and N1 atoms have net negative charge. As Q17 is displaced in the positive direction, the O atoms move closer to the C and N1 atoms, increasing coulombic repulsion. To summarize, the major contribution to the potential surface when Q17 moves in the negative direction is breaking of the N-N partial pi bond. The major



contribution to the potential surface when Q17 moves in the positive direction is increasing coulombic repulsion.

### Coordinate 14

Internal coordinate 14 (Q14) is the motion of N2 out of the CN1C plane. This motion is similar to ammonia inversion and defines angle  $\beta$  of Figure 3-1. Table 3-4 shows the energy and geometry changes as Q14 varies from 0°, the planar geometry, to 46°. The potential surface is symmetric about 0°. The 6-31G\* inversion barrier height is 406 cal/mole and the 4-21NO\* inversion barrier height is 1603 cal/mole. The true inversion barrier height should be between these two values and is probably closer to the 6-31G\* value. These results confirm the conclusion in Chapter 2 that the 4-21NO\* basis set overestimates inversion barrier heights.

The energy values given in Table 3-4 were fitted to fourth order and sixth order even polynomials. The results of the fourth order fit are given in equation 3-2 and as the dashed line in Figure 3-14. The standard deviation of equation 3-2 is 15 cal/mole. The results of the sixth order



$$V(x)=0.418 -0.1063E-02x^2+0.6603E-06x^4 \quad (3-2)$$

$$V(x)=0.405 -0.9092E-03x^2+0.4518E-06x^4 +0.6643E-10x^6 \quad (3-3)$$

V the potential energy in kcal/mole.

x the value of coordinate 14 in degrees.

fit are given in equation 3-3 and as the dashed line in Figure 3-15.

The standard deviation of equation 3-3 is less than 1 cal/mole.

Figures 3-14 and 3-15 show that Q14, which defines angle  $\beta$  in Figure 3-1, changes the potential energy by less than 400 cal/mole as it varies from 0 to  $\pm 40^\circ$ . The double well and low potential energy associated with Q14 make it very responsive to minor changes in the crystal environment as shown by Gilardi's review [10].

The eigenvalues of the quartic oscillator given in equation (3-2) provide the basis for an explanation of the observed dimethyl nitramine structural changes. These eigenvalues are obtained by transforming the equation to atomic units and changing Q14 to a mass-weighted frame. Expansion with sixty harmonic oscillator basis functions gives the lowest seven eigenvalues as 318, 548, 1169, 1852, 2653, 3540 and 4501 cal/mole. The lowest eigenvalue is below the barrier. The ground state wavefunction may, therefore, be localized in either the left or right well. This splits the wavefunction



TABLE 3-4<sup>a</sup>Coordinate 14<sup>b</sup>

| Q14 <sup>c</sup> | Delta E <sup>d</sup> | N2-N1 | N-O   | C-N   |
|------------------|----------------------|-------|-------|-------|
| 0.1              | .406                 | 1.326 | 1.200 | 1.452 |
| 8.7              | .338                 | 1.327 | 1.200 | 1.453 |
| 20.2             | .114                 | 1.335 | 1.198 | 1.453 |
| 28.8             | 0.00                 | 1.343 | 1.197 | 1.455 |
| 37.4             | .200                 | 1.356 | 1.195 | 1.458 |
| 46.0             | 1.134                | 1.372 | 1.193 | 1.462 |
| Q14              | NNO                  | ONO   | CNN   | CNC   |
| 0.1              | 117.3                | 125.3 | 117.4 | 125.1 |
| 8.7              | 117.3                | 125.3 | 117.3 | 124.7 |
| 20.2             | 117.4                | 125.3 | 116.8 | 122.6 |
| 28.8             | 117.4                | 125.2 | 115.8 | 120.4 |
| 37.4             | 117.4                | 125.2 | 114.3 | 117.7 |
| 46.0             | 117.4                | 125.1 | 111.9 | 115   |

a. Bond lengths in angstroms. Bond angles in degrees.

b. See Figure 3-1 for the definition of Q14.

c. The angle between the NN bond and its projection on the CNC plane in degrees.

d. Energy difference in kcal/mole.



FIGURE 3-14  
Q14 POWER SERIES TO  $X^4$

52

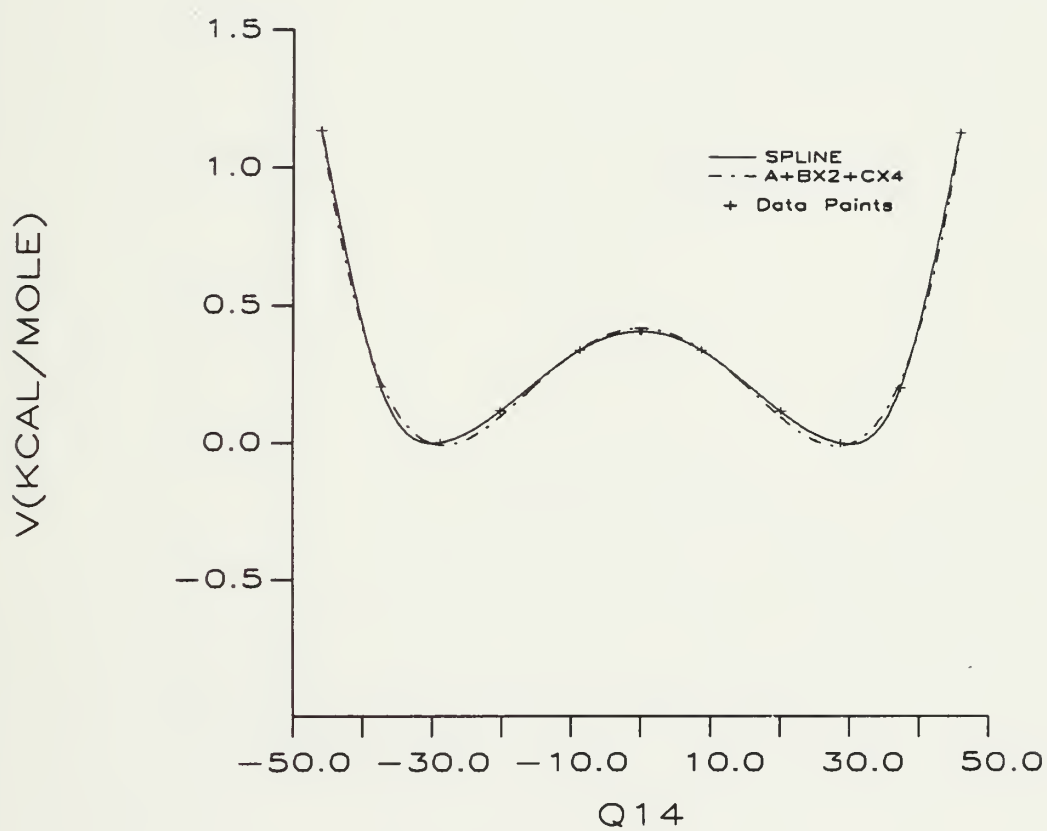




FIGURE 3-15  
Q14 POWER SERIES TO  $X^6$

53

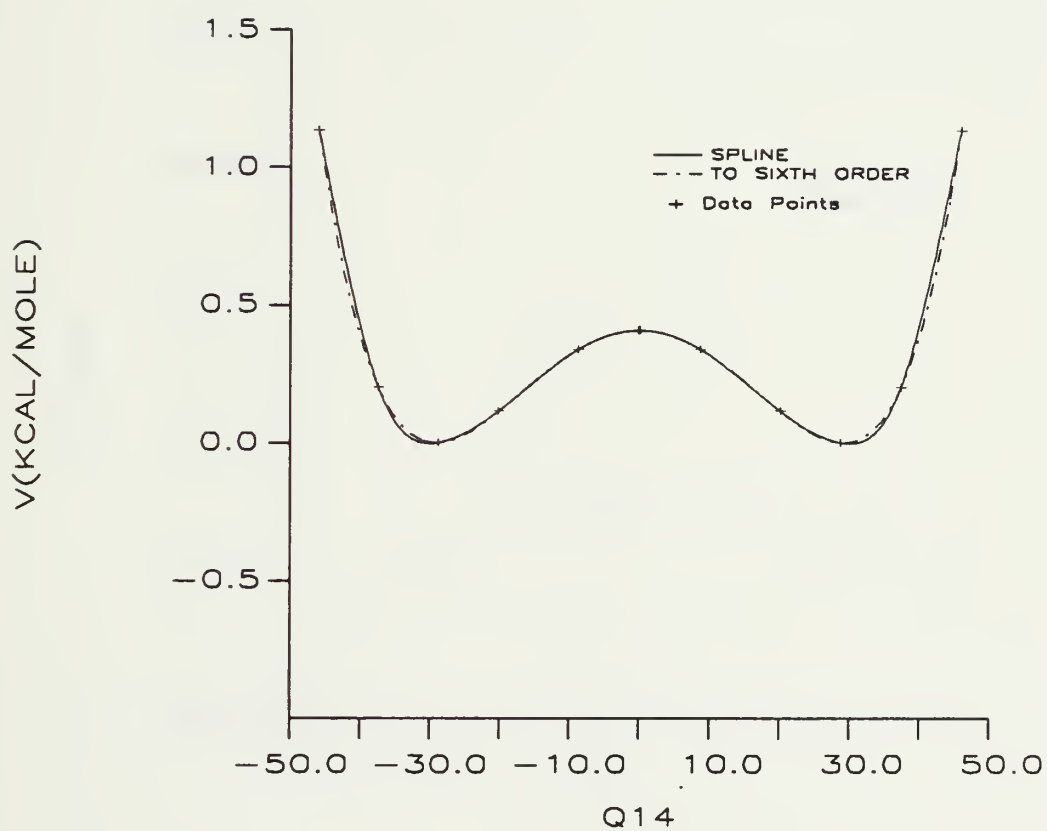




FIGURE 3-16  
Q14 ONO

54

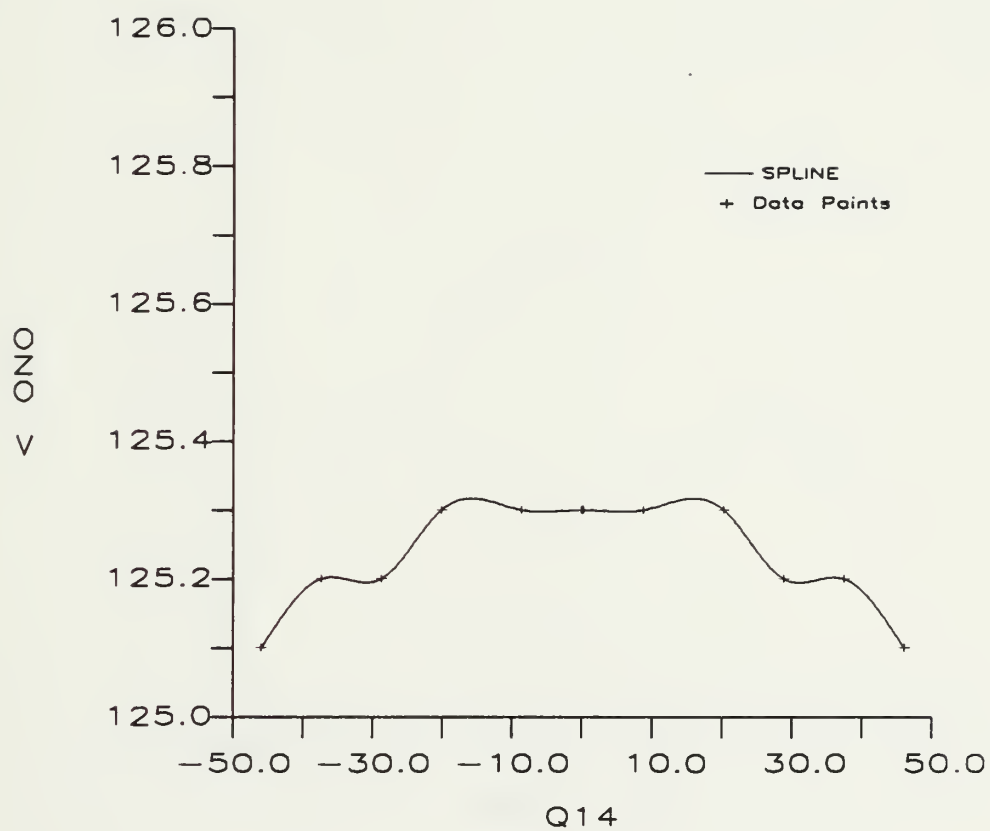




FIGURE 3-17  
Q14 ONN

55

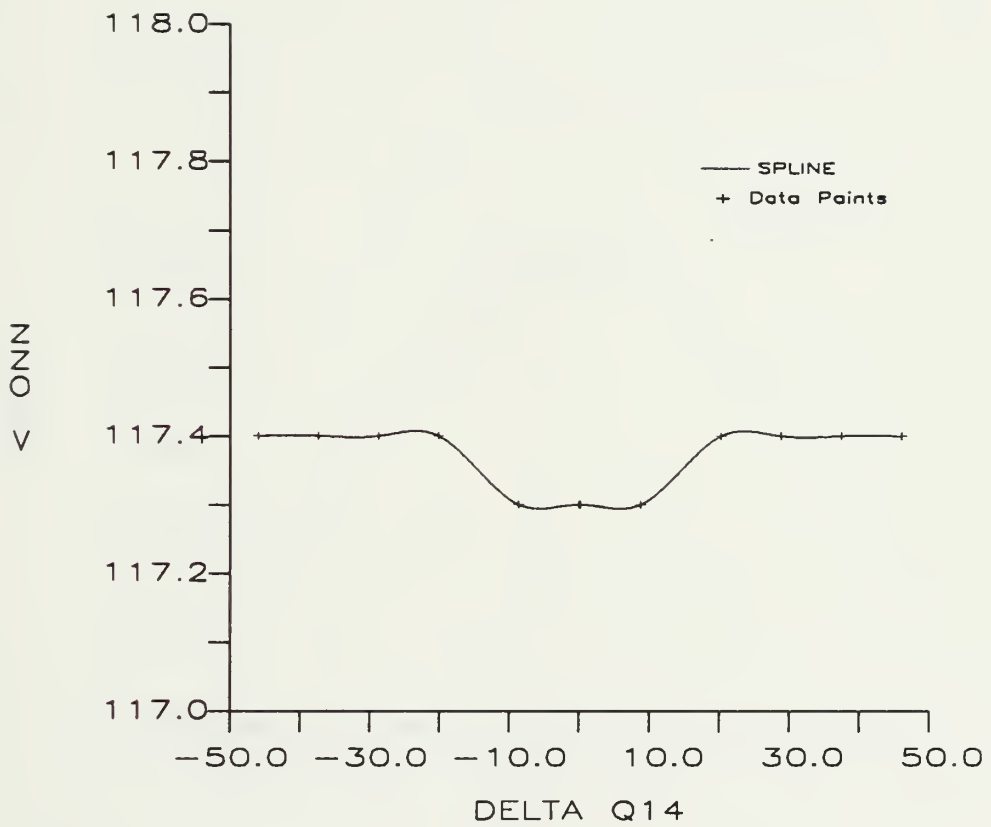




FIGURE 3-18  
Q14 NO

56

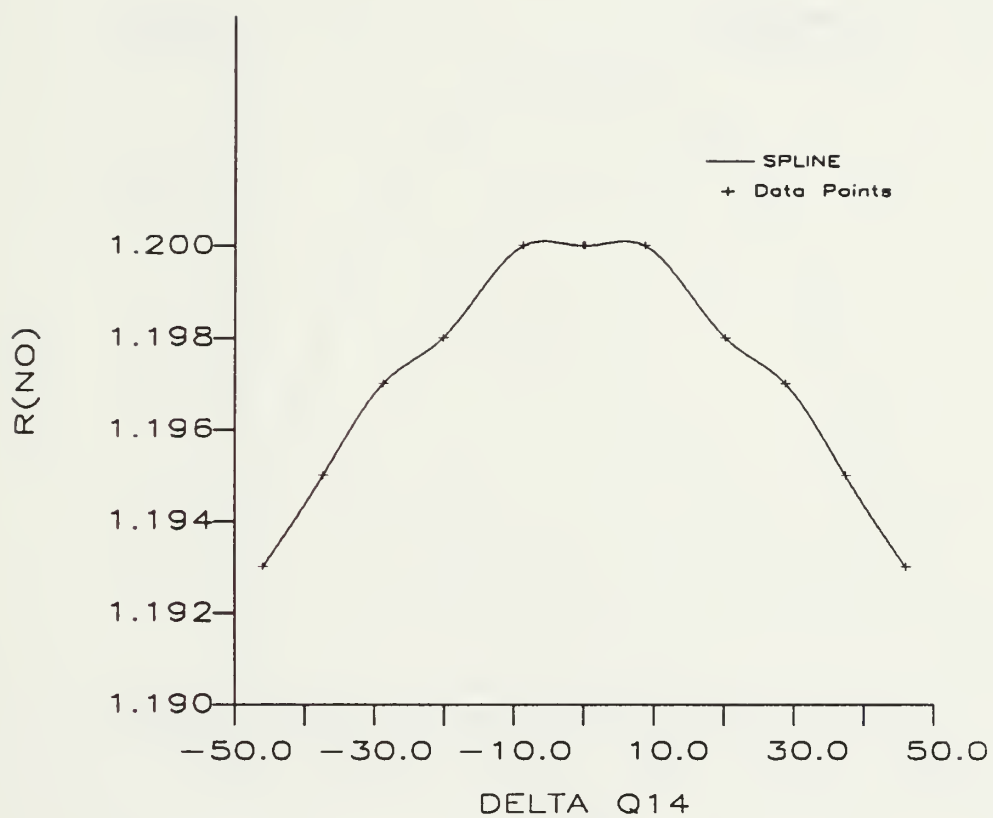




FIGURE 3-19  
Q14 CNN

57

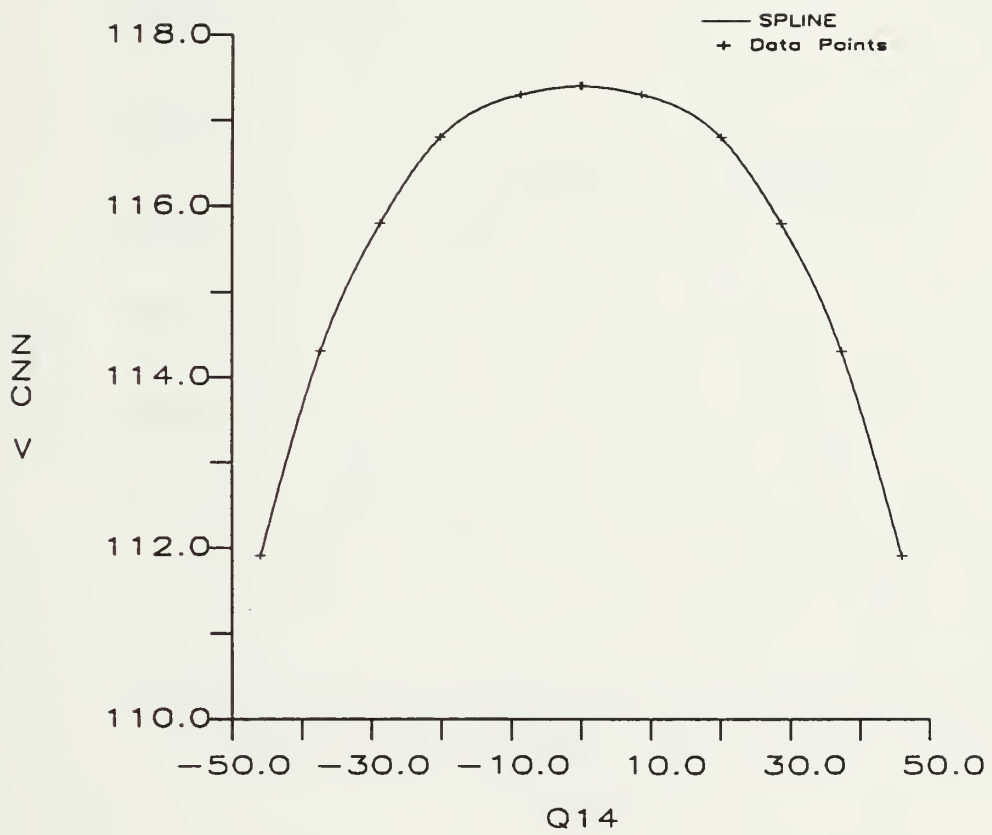




FIGURE 3-20  
Q14 CNC

58

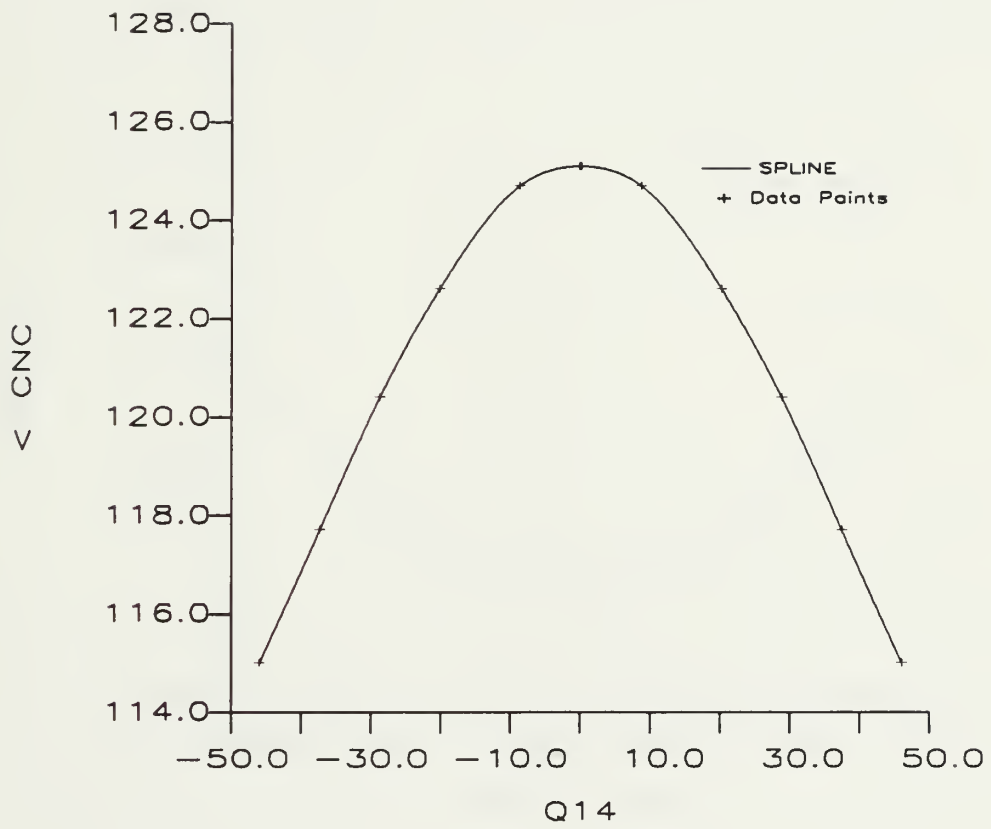




FIGURE 3-21  
Q14 N-N

59

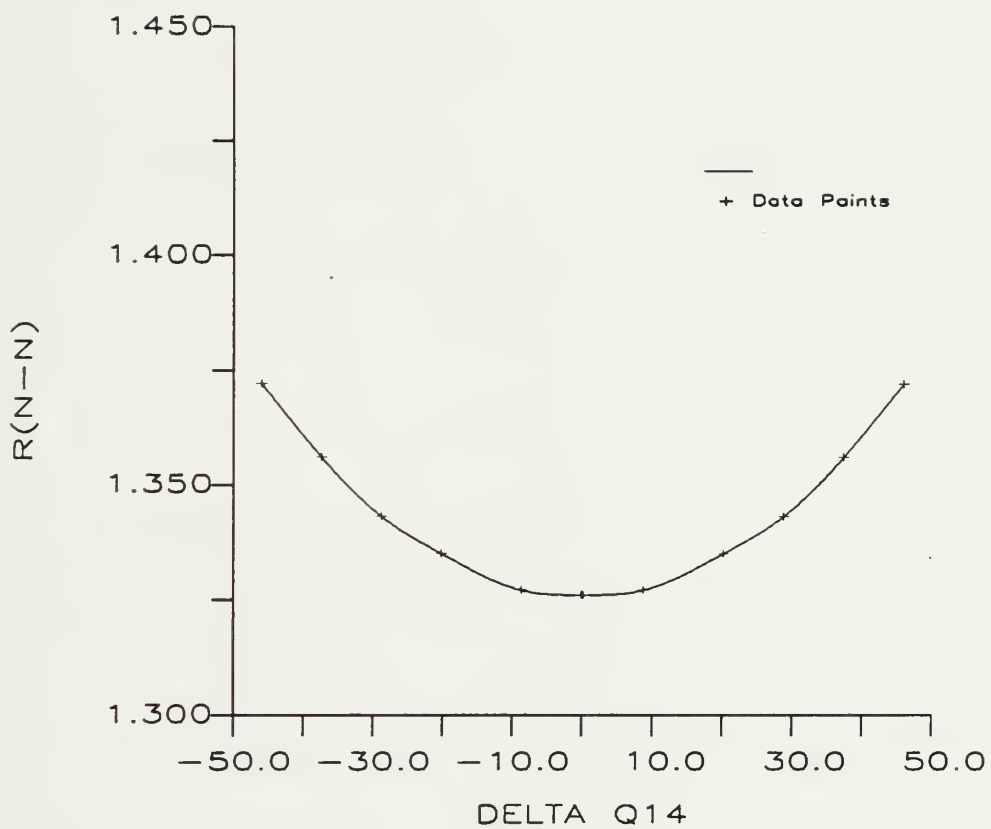
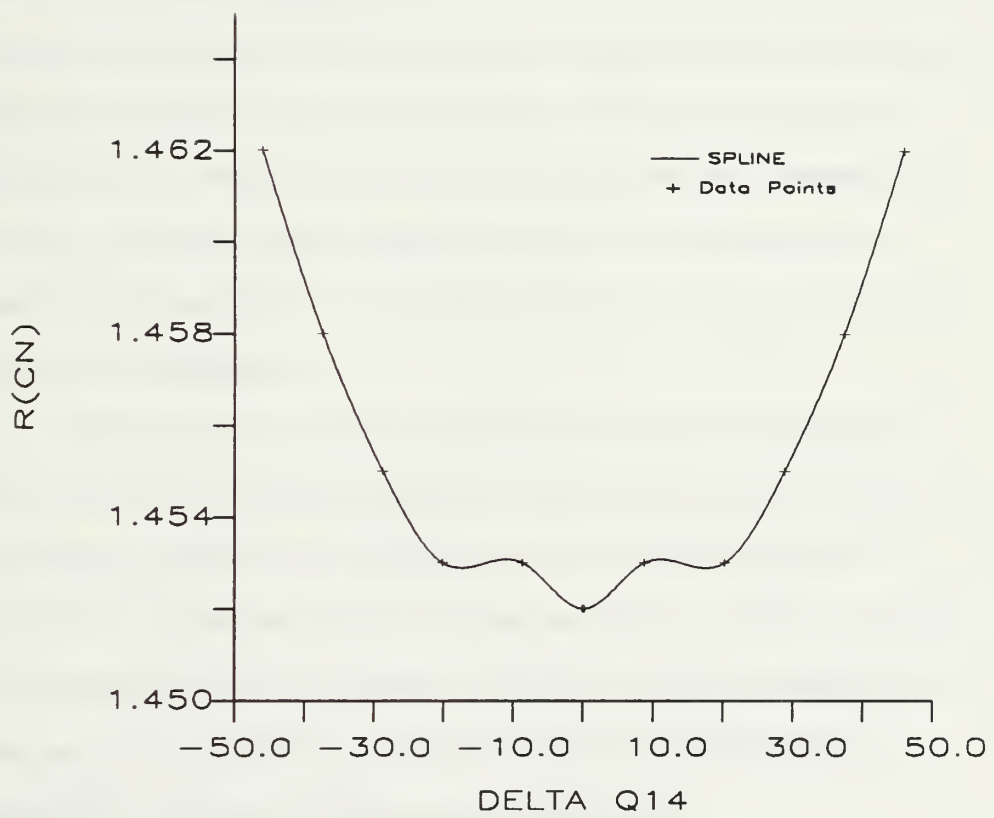




FIGURE 3-22  
Q14 CN

6C





into plus and minus symmetry groups and should give a complicated vibrational spectrum.

X-ray and neutron diffraction experiments determine bond lengths and bond angles by measuring the distance between maxima in the motion-averaged electron or nuclear density function. If we assume Boltzmann statistics, at the 107 K transition temperature 74% of the molecules are in the Q14 vibrational ground state while 26% of the molecules are in planar excited states. The observation of a planar structure means that the rate of interconversion between the ground and excited state occurs faster than the experiment can measure. All molecules are, therefore, effectively planar above the transition temperature.

The electron diffraction experiment for dimethyl nitramine is conducted at a temperature greater than the melting point of 331 K. If we assume a Boltzmann distribution of Q14 vibrational states, the populations of the lowest five state are;  $v=0$  47%,  $v=1$  33%,  $v=2$  13%,  $v=3$  5% and  $v=4$  1%. The electron diffraction experiment observes a mixture of several different vibrational states with almost equal populations of planar and non-planar geometries.

The geometry changes associated with changing Q14 are shown in Figures 3-16 through 3-22. Figures 3-16 and 3-17 show that the ONO and ONN angles are almost constant over the range of Q14 considered here. Figures 3-18, 3-19 and 3-20 show that the



change in the NO bond length, the CNN angle and the CNC angle have the same functional form. The values of these parameters become smaller as the Q14 becomes larger in magnitude. Figures 3-21 and 3-22 show that the N-N and C-N bond lengths are at a minimum when Q14 equals zero and become longer as Q14 increases in magnitude. All of these geometry changes reflect the change in bonding around N1 from  $sp^2$  at the planar geometry to  $sp^3$  as Q14 increases in magnitude.

### Coordinate 28

Coordinate 28, torsion of the N-N bond, is defined as  $(T_{4216} + T_{3215})/2$  in this work.  $T_{4216}$  is the angle between the O4, N2 and N1 plane and the N2, N1 and C6 plane.  $T_{3215}$  is similarly defined. Determining the torsional potential surface answers the question; Is the dimethyl nitramine torsion like nitromethane with free internal rotation or is it like ethylene with a more rigid structure? Because the N1 lone pair forms a partial pi bond, we might expect dimethyl nitramine to be similar to ethylene.

Table 3-5 summarizes the energy and geometry changes as Q28 varies from  $0^\circ$  to  $180^\circ$ . Figure 3-23 shows a plot of the energy changes and the twofold potential function,  $V_0/2(1 - \cos(2x))$ , with  $V_0 = 11.35$  kcal/mole. The 4-21NO\* basis set determines  $V_0 = 10.39$



kcal/mole, confirming that the 4-21NO\* basis set underestimates rotational barrier heights around nitrogen.

The twofold term dominates the dimethyl nitramine torsional potential function. A pure twofold description of the potential function is inadequate, however, because it does not have enough curvature near 0° or 180°. Figure 3-24 and equation 3-4 give the results of a least squares fit to a potential function with a twofold and a fourfold term. Figure 3-25 and equation 3-5 give the results of a least squares fit to potential function with a twofold and a sixfold term. The potential function containing the fourfold term provides a better description of the torsional

$$V(x)=5.692(1-\cos(2x))+.332(1-\cos(4x)) \quad (3-4)$$

standard deviation = .282

$$V(x)=5.782(1-\cos(2x))+.192(1-\cos(6x)) \quad (3-5)$$

standard deviation = .343

$$V(x)=5.191(1-\cos(2x))+0.479(1-\cos(4x)) \quad (3-6)$$

standard deviation = .162.

V = the potential energy in kcal/mole.

x = the value of Q28 in degrees.



potential surface. Equation 3-6 is the result of a least squares fit to the 4-21NO\* data using a twofold and a fourfold basis. The ratio of the fourfold coefficient,  $V_4$ , to the twofold coefficient,  $V_2$ , which gives an estimate of how the potential surface deviates from a pure twofold function, is .0583 for results from the 6-31G\* basis set and .0922 for results from the 4-21NO\* basis set. The 4-21NO\* results are not as reliable as the 6-31G\* results because fewer data points are available for the least squares fit, but it appears that the 4-21NO\* basis overestimates the contribution of the four-fold term.

Rotation of Q28 breaks the  $C_s$  symmetry plane. As a result, the N-O bonds experience different environments during rotation. Figure 3-26 shows the change in the N2-O3 bond as a function of Q28. From 0° to 180° the N2-O3 bond is cis to the CN bonds and from 180° to 360° the bond is cis to the N1 lone pair. Interaction between the CN and NO bonds prevents shortening of the NO bond. The NO bond appears to have very little interaction with the N1 lone pair and shortens significantly.

Figure 3-27 shows that the change in the CN bond length is not a smooth sinusoidal function of Q28. The maxima occur at the normal positions of 90° and 270°, but the minima occur at about 25° and 205° instead of 0° and 180°. The minima occur when the NO bond eclipses one of the CN bonds.



TABLE 3-5<sup>a</sup>  
Coordinate 28

| Q28 <sup>b</sup> | Delta E <sup>c</sup> | N-N   | O3-N2    | O4-N2    |          |
|------------------|----------------------|-------|----------|----------|----------|
| 0.0              | 0                    | 1.343 | 1.197    | 1.197    |          |
| -22.6            | 2.270                | 1.362 | 1.193    | 1.194    |          |
| 25.0             | 2.624                | 1.366 | 1.193    | 1.193    |          |
| 40.2             | 5.613                | 1.386 | 1.192    | 1.189    |          |
| 62.8             | 9.531                | 1.412 | 1.192    | 1.184    |          |
| 91.6             | 11.337               | 1.424 | 1.192    | 1.181    |          |
| 113.6            | 9.965                | 1.413 | 1.192    | 1.183    |          |
| 142.9            | 3.947                | 1.374 | 1.193    | 1.191    |          |
| 157.7            | 2.155                | 1.364 | 1.194    | 1.193    |          |
| Q28              | C5-N1                | C6-N1 | O3-N2-N1 | O4-N2-N1 | O4-N2-O3 |
| 0.0              | 1.455                | 1.455 | 117.4    | 117.4    | 125.2    |
| -22.6            | 1.459                | 1.454 | 116.9    | 117.8    | 125.4    |
| 25.0             | 1.454                | 1.458 | 117.8    | 116.8    | 125.3    |
| 40.2             | 1.455                | 1.460 | 118.2    | 116.1    | 125.7    |
| 62.8             | 1.458                | 1.461 | 118.3    | 115.7    | 126.1    |
| 91.6             | 1.461                | 1.461 | 117.9    | 115.9    | 126.2    |
| 113.6            | 1.460                | 1.458 | 118.1    | 115.7    | 126.1    |
| 142.9            | 1.459                | 1.454 | 118      | 116.5    | 125.5    |
| 157.7            | 1.458                | 1.454 | 117.7    | 117      | 125.3    |



| Q28   | C5-N1-N2 | C6-N1-N2 | C6-N1-C5 |
|-------|----------|----------|----------|
| 0.0   | 115.8    | 115.8    | 120.4    |
| -22.6 | 113.8    | 114.3    | 117.4    |
| 25.0  | 114.5    | 114      | 116.9    |
| 40.2  | 113.2    | 111.5    | 115.3    |
| 62.8  | 111.1    | 108.3    | 113.8    |
| 91.6  | 108.6    | 108.8    | 113.4    |
| 113.6 | 108.4    | 110.8    | 113.7    |
| 142.9 | 113.0    | 113.9    | 116.0    |
| 157.7 | 114.3    | 114.6    | 117.0    |

- Bond lengths in angstroms. Bond angles in degrees.
- Coordinate 28,  $(T(4216)+T(3215))/2$ , in degrees.
- Energy difference in kcal/mole.



FIGURE 3-23  
Q28 COS(2\*THETA)

67

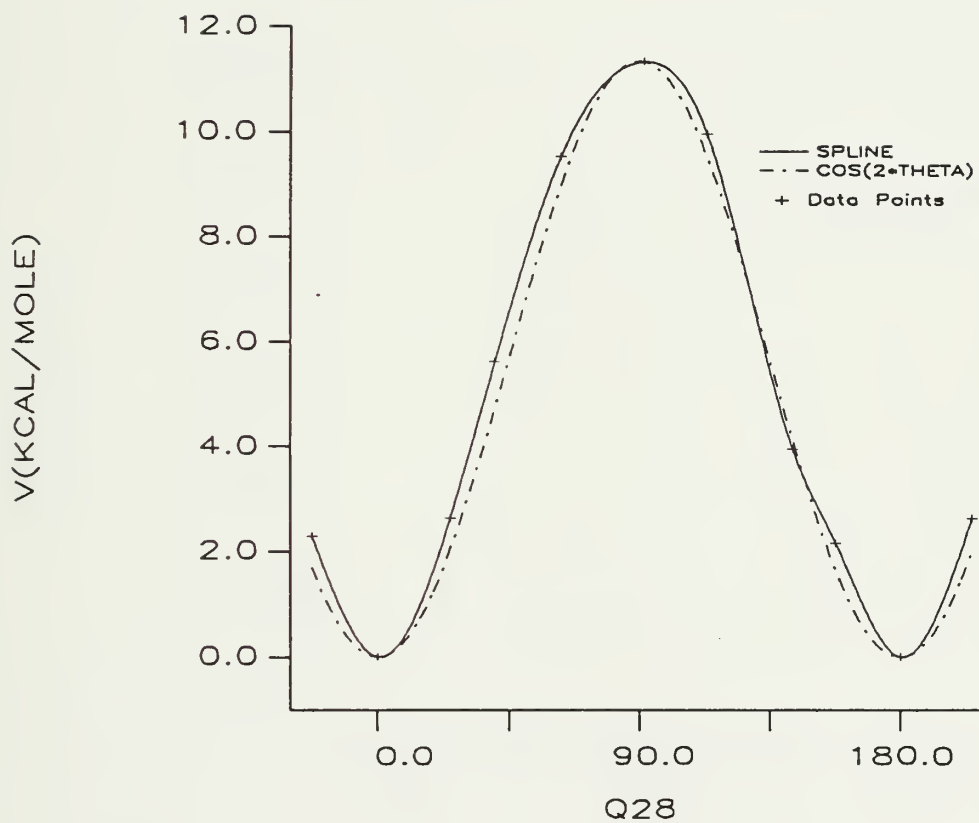




FIGURE 3-24  
Q28  $\cos(2 \cdot \text{THETA}) + \cos(4 \cdot \text{THETA})$

68

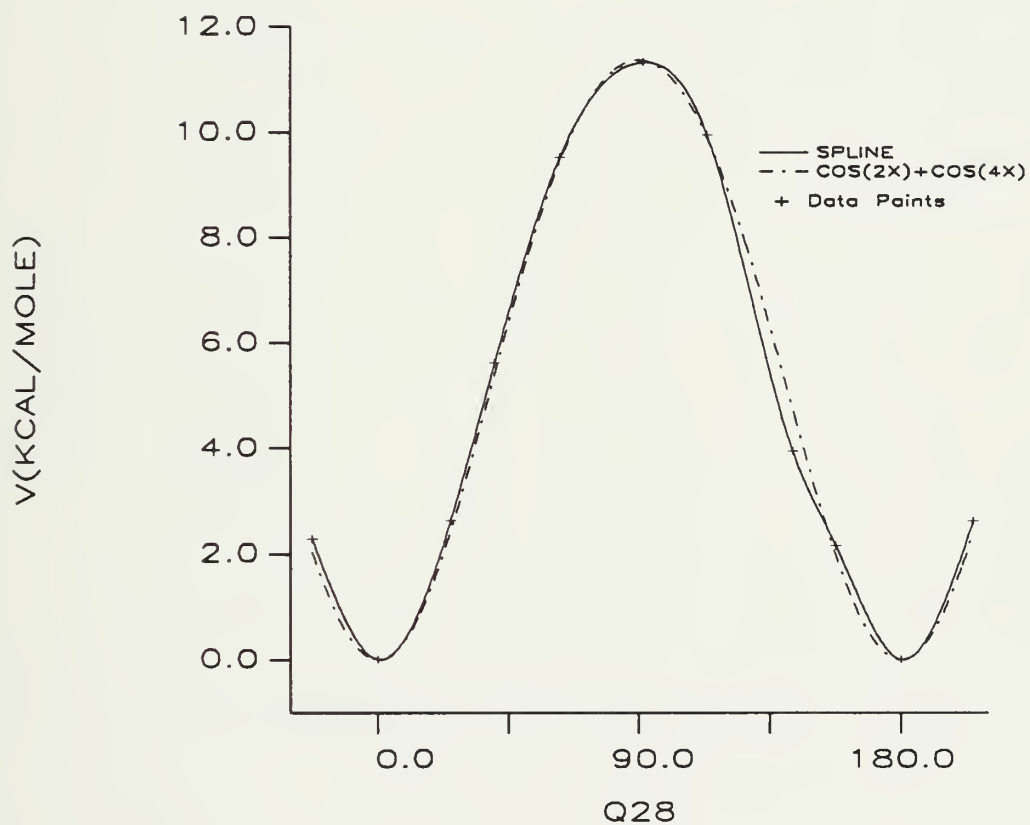




FIGURE 3-25  
Q28  $\cos(2*\text{THETA}) + \cos(6*\text{THETA})$

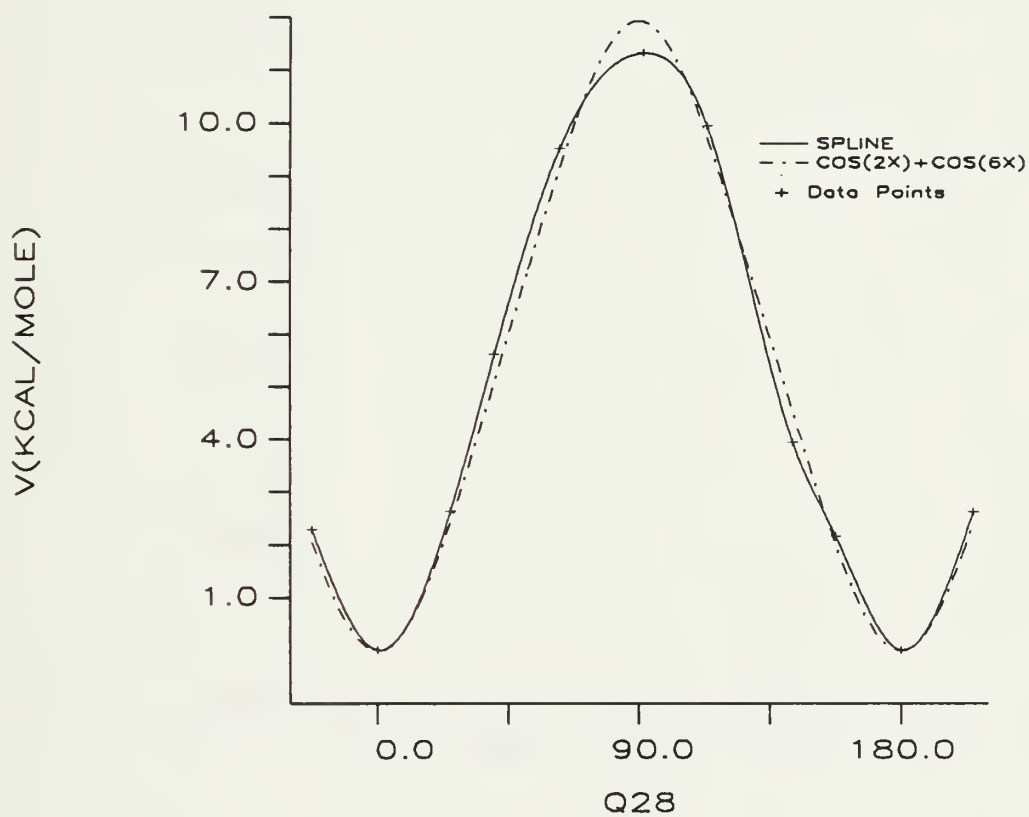




FIGURE 3-26  
Q28 N-O

7C

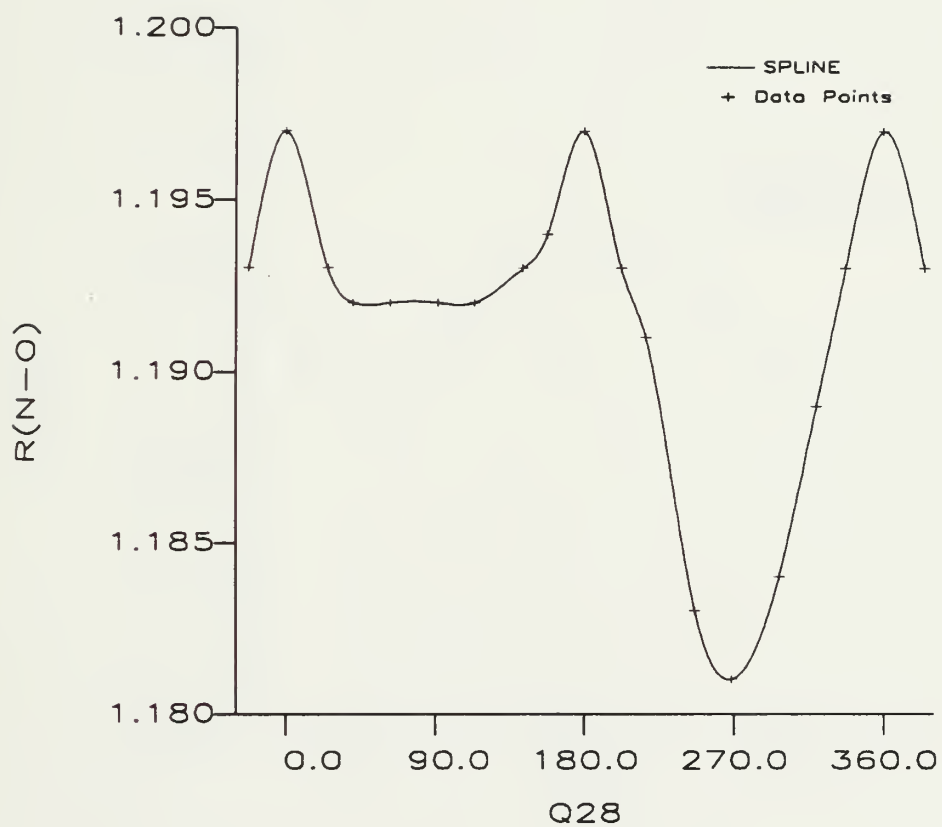




FIGURE 3-27  
Q28 C-N

71

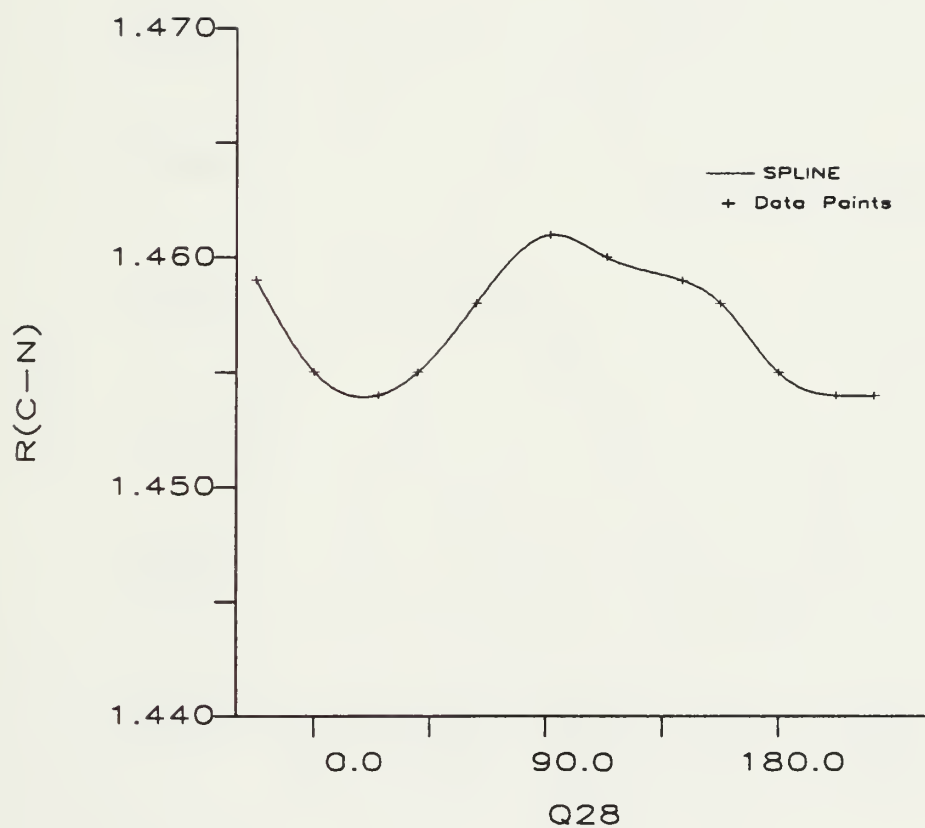




FIGURE 3-28  
Q28 <NNO

72

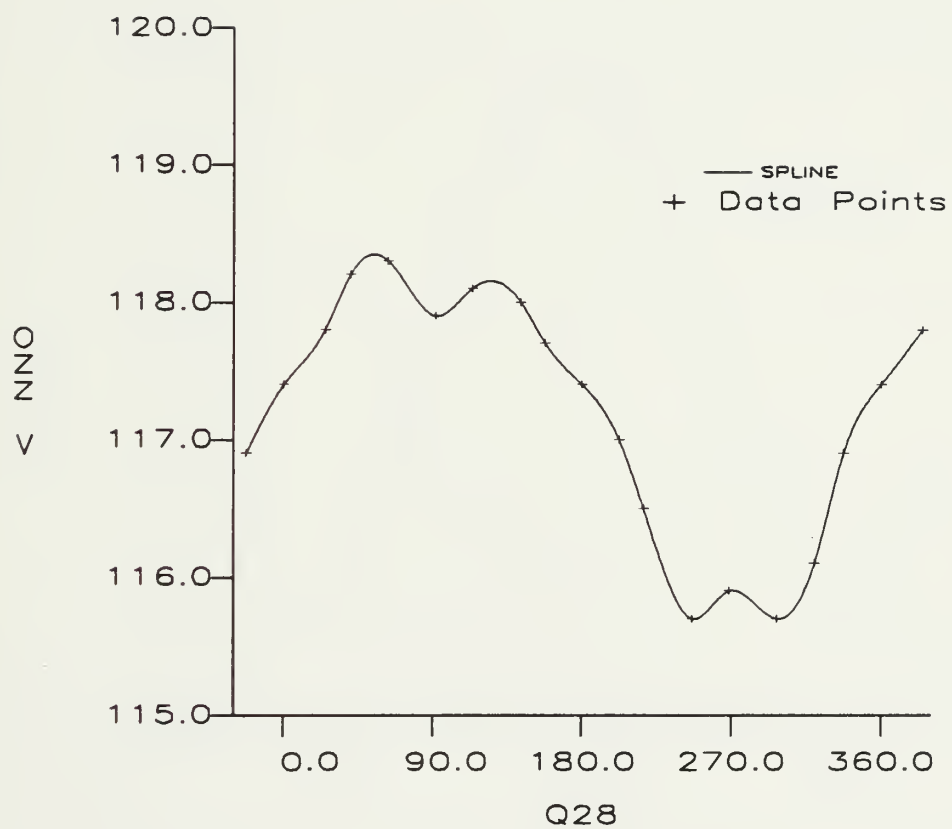




FIGURE 3-29  
Q28 N-N

73

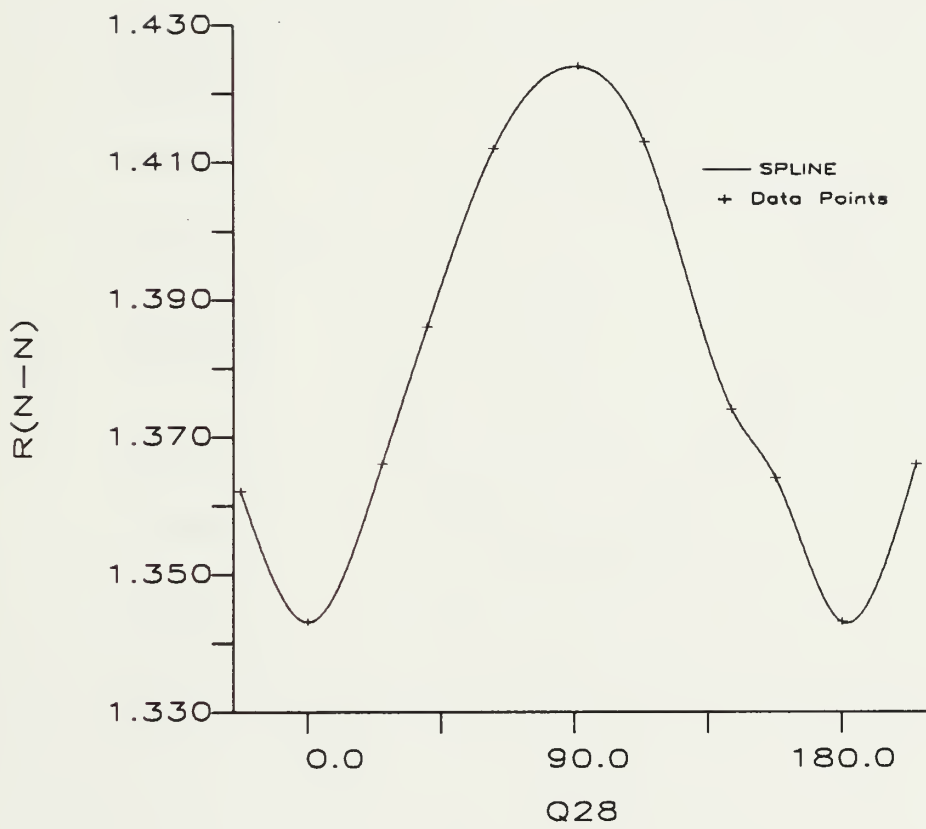




FIGURE 3-30  
Q28 <CNC

74

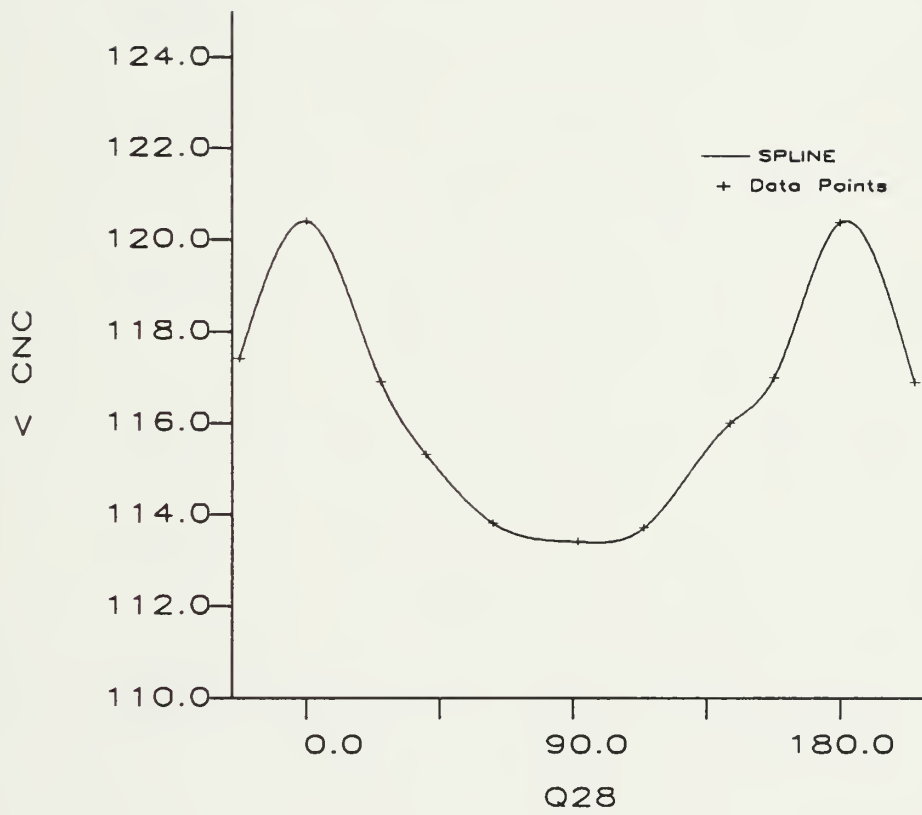




FIGURE 3-31  
Q28 <ONO

75

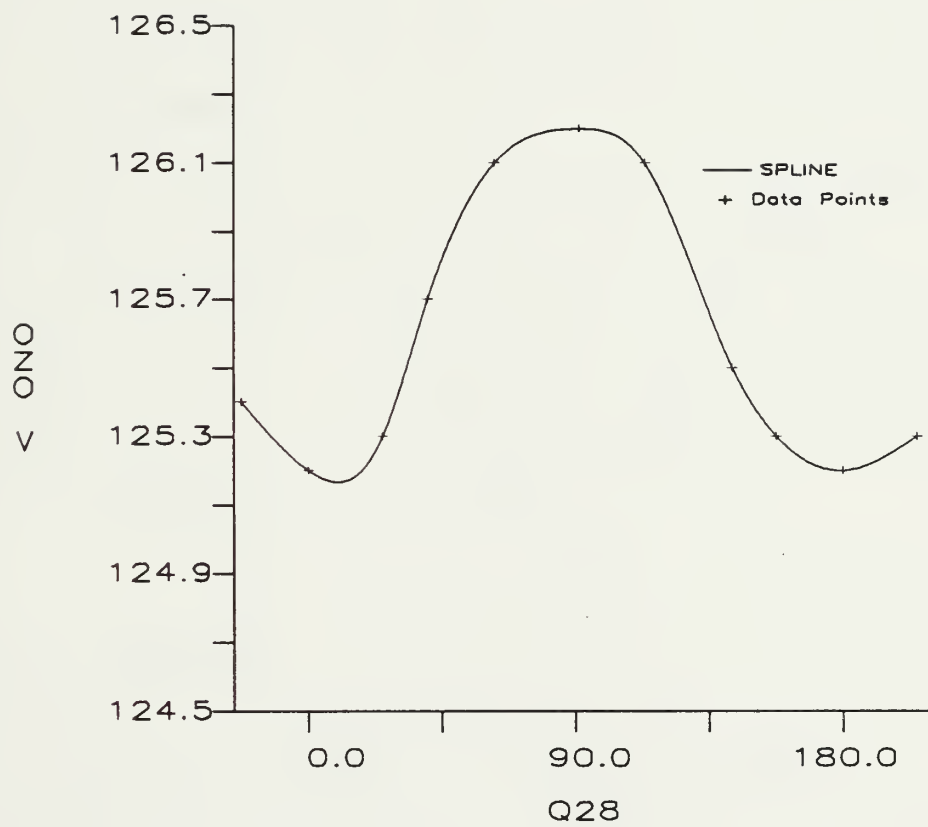




FIGURE 3-32  
Q28 < CNN

76

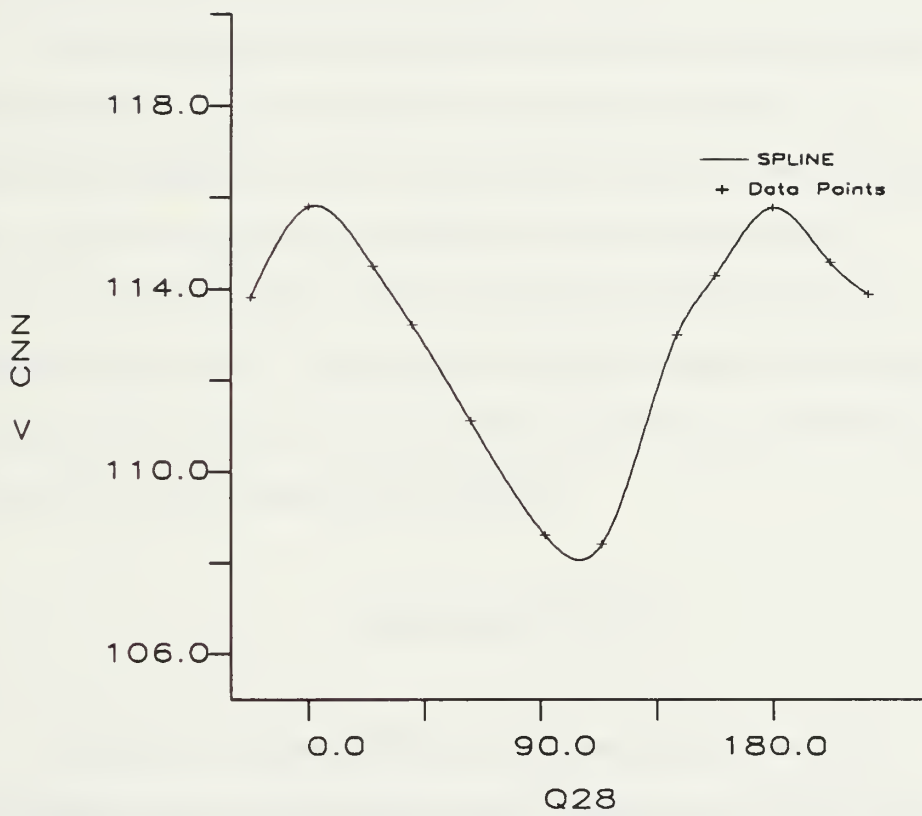




Figure 3-28 shows the change in the NNO3 bond angle as a function of Q28. The NNO angle has a curious double hump near 90° and again near 270°. The maxima and minima are offset by about +/- 30° from the symmetric maxima and minima values. The positions of the maxima and minima do not correspond to significant structural interactions and their origin is baffling.

Figures 3-29, 3-30, 3-31 and 3-32 show the changes in the N-N bond length and the CNC, ONO and CNN bond angles. The geometry changes are those expected from a molecule with a twofold axis. The N-N bond length and ONO bond angle pass through maxima at the 90° position, while the CNC and CNN bond angles pass through minima. These geometry changes reflect the change in N1 bonding from nearly  $sp^2$  at the optimum geometry to  $sp^3$  as the partial N-N pi bond breaks during rotation.

### Concluding Remarks

The two out-of-plane and one torsional potential surfaces calculated in this Chapter can be used to improve the model used to predict the density of unknown molecules that contain the nitramine group. The equilibrium nitramine geometry is non-planar. The inversion barrier is about 400 cal/mole resulting in free inversion at very low temperatures. The N-N torsional motion is dominated by a



two-fold term and the barrier height is predicted to be 11.35 kcal/mole by the 6-31G\* basis set. The bonding at N1 is a delicate balance between configurations that may be classically described as  $sp^2$  and  $sp^3$  hybrids.



## CHAPTER FOUR

### Conclusion

In this study a thorough ab initio study of dimethyl nitramine was presented. In addition a thorough review of basis set effects for the 4-21NO\* and 6-31G\* basis sets and an extension of a previous study [12] on formamide were given. In this chapter, a few of the more important results are summarized and suggestions for future work are offered.

Polarization functions are absolutely necessary for a proper description of nitrogen and oxygen. This point has been demonstrated in previous studies [12,14,15,25] and the results of this study confirm this earlier conclusion. If polarization functions are not included in the basis set, dimethyl nitramine is incorrectly predicted to be planar.

The 4-21NO\* basis set provides an economical means for calculations on large molecules, but it has some important limitations. The basis set tends to overestimate the pyramidal nature of nitrogen, overestimate nitrogen inversion barriers and underestimate nitrogen rotation barriers. This difficulty is very apparent for low energy motions.

The popular 6-31G\* basis set [13] is more balanced than the 4-21NO\* basis set, but this study has shown it has some unexpected limitations. This basis set incorrectly predicts formamide to be planar. Although, formamide is a very severe test of any theoretical method,



this result shows that the 6-31G\* basis set tends to underestimate the pyramidal nature of nitrogen. Adding p functions to hydrogen improves the situation, but the formamide structure is still predicted to be too flat. The 6-31G\* rotation and inversion barriers are in almost perfect agreement with 6-311G\*\*/MP2 values.

Caution should be exercised when interpreting the results of analytical force constant and frequency calculations from GAUSSIAN 82 [21] singlet ground state UHF wavefunctions. For azamethine ylide the UHF wavefunction determined multiple imaginary frequencies for a geometry that the RHF wavefunction showed to be the ground state [22]. The cause of this difficulty is unknown.

Dimethyl nitramine is predicted to be non-planar by both the 4-21NO\* and 6-31G\* basis sets. The barrier to inversion of the methyl groups is predicted to be 406 cal/mole by the 6-31G\* basis set. The  $v=0$  vibrational state is below the barrier while all other vibrational states are above the barrier. The first excited inversion vibrational state is about 230 cal/mole above the ground state. The molecule freely inverts at very low temperatures. Electron diffraction studies, conducted at or above the melting point of 331 K, observe several different vibrational states with over half of the molecules in planar excited states. The N-N rotation barrier is essentially twofold with a barrier of about 11.35 kcal/mole. The bonding at the amine nitrogen is a delicate balance between states that may be described as classical  $sp^2$  and  $sp^3$  states.



A comprehensive comparison of ab initio and experimental rotation and inversion potential surfaces needs to be completed. The Scaled Quantum Mechanical Force Field method [36] is a sophisticated method that corrects problems in the ab initio calculation of harmonic vibrational potential surfaces. Although ab initio calculations provide reasonable agreement with experimental rotation and inversion barriers, ab initio energy eigenvalues do not give very good agreement with observed energy separations [37]. A study into the reasons for this discrepancy would be very helpful.

As stated in Chapter Two, this study made the assumption that the contribution of the lowest excited state determinant to the NO<sub>2</sub> wavefunction is constant from molecule to molecule. An MCSCF study over a series of NO<sub>2</sub> and NNO<sub>2</sub> containing molecules should be completed to test this assumption.



## APPENDIX

# FUNPLOT PROGRAM DESCRIPTION

The FUNPLOT program provides easy and rapid data analysis. The program fits data with the following functions; cubic spline, linear least squares and least squares to user supplied basis functions. A known function may also be plotted with the program.

FUNPLOT uses the DI-3000 GRAFMAKER and IMSL libraries. The program sends the plot commands to a device-independent file called the metafile which is disposed to the VAX 8600. The metafile commands are translated to device-specific commands by the metafile translator.

The following JCL is used to execute the program.

```
JOB,JN=<>,T=15.
```

```
ACCOUNT,US=<>,UPW=<>.
```

```
ACCESS,DN=FUNPLOT,PDN=FUNPLOT,
```

```
OWN=CMAO273.
```

```
FETCH,DN=BASIS,TEXT='<>'. ; only if least squares  
fitting to a set of user supplied basis functions is  
desired.
```

```
CFT,I=BASIS,L=0.
```



FETCH,DN=VPOT,TEXT='<>'. ; only if plotting a user  
supplied function.

CFT,I=VPOT,L=0.

ASSIGN,DN=\$IN,A=FT05. ; input deck

ASSIGN,DN=\$OUT,A=FT06. ; output deck

LIB,DN=DI3LIB:GRAFLIB. ; get DI3000 libraries.

LIB,DN=IMSL. ; get IMSL library.

CFT,I=FUNPLOT,L=0.

LDR,LIB=DI3LIB:GRAFLIB:IMSLIB. ; execute the  
program.

ACCESS,DN=METAPLT. ; get the metafile from CRAY  
permanent disk file.

DISPOSE,DN=METAPLT,TEXT='<>'. ; send the metafile  
to the VAX 8600.

/EOF

<INPUT DECK>

The following is the input description for the program  
FUNPLOT.

**CARD ONE:** IDATA (format I2)

IDATA is the number of input data points. The maximum  
number of data points is 50.



**CARD SET TWO:** X(I),Y(I) Free format, list directed input.

Enter the data points as real numbers. IDATA pairs must be entered or the program will abort.

**CARD THREE:** TITLE, XNOTE, YNOTE, TXTHGT (format A40, 3F10.6)

TITLE is an arbitrary string. The first and last characters of the string are interpreted as delimiters by the DI-3000 package. DI-3000 will issue a run time abort if the first and last characters are not the same. The character \$ is recommended as a delimiter.

XNOTE, YNOTE position the title string. The title is vertically and horizontally centered at XNOTE, YNOTE. The position is described in terms of **Chart Space Coordinates**. The Chart Space runs from (0,0), the lower left corner, to (1000,1000), the upper right corner. The default position for the title is (500,950).

TXTHGT is the height of the characters in the title in **Chart Space Coordinates**. The default size of the characters is 40.

**CARD FOUR:** XTITLE, XMIN, XMAX, TIC, TXTHGT  
(format A30, 2F10.6, A3, 7X, F10.6)



XTITLE is the title for the X-axis. The first and last characters are interpreted as string delimiters by DI-3000.

XMIN is the minimum value on the X-axis.

XMAX is the maximum value on the X-axis. If XMIN=XMAX, DI-3000 determines the range of the x-axis.

TIC If the control word TIC is not present, DI-3000 automatically determines the range of the X-axis. If the control word TIC is present, the following card must follow each axis definition card.

TSTART,TEND,TINCR,ISTR,ICYC,LFWDTH,LFMT  
format (3E10.3,3I5,A30)

TSTART The value for the first tic mark on an axis.

TEND The value for the last tic mark on an axis.

TINCR The distance between tic marks.

ISTR Number of the first tic mark to be labeled. For example, if ISTR equals 3, the first two tic marks are not labeled. The default value is 1.

ICYC Determines the tic mark labeling pattern. If ICYC equals 1, every tic mark is labeled. If ICYC equals 2, every other tic mark is labeled. The default value is 2.

LFWDTH The number of characters in the tic mark format specification. If LFMT is \$(F5.1)\$,



LFWDTH equals 5. If LFMT is \$(F5.1,2X)\$,

LFWDTH equals 7.

LFMT The tic mark label format. The format specification must be a delimited DI-3000 text string and must be enclosed in parentheses. The above examples for LFMT are in the correct format. Y-axis labels should be offset by two characters, use formats like \$(E10.3,2X)\$, so that the tic marks are not overwritten.

TXTHGT has the same meaning as in Card 4.

**CARD FIVE:** YTITLE,YMIN,YMAX,TIC (format A30,2F10.6,A3)

The variables are analogous to the X-axis variables.

**CARD SIX:** NPLOTS,XNOTE,YNOTE,TXTHGT (format I1,9X,3F10.1)

NPLOTS is the number of curves to be drawn.

XNOTE,YNOTE fix the lower left corner of the legend box.

Legends, DTITLE on card 7, are assigned to each curve and are placed in the legend box. By default, the legend box is in the upper right corner of the chart.

TXTHGT is the same as for card 4. The default legend text height is 20.



**CARD SEVEN:** PLTTYP,DTITLE (format A6,A20)

Cards seven and eight are repeated NPLOTS times. PLTTYP is the type of curve to be drawn. The following keywords are recognized:

**MARK** plot marks on the input data points.

**SPLINE** fit a natural cubic spline to the data points.

The cubic splines data points are printed in the output file.

**LEAST** perform a linear least squares fit to the data.

The least squares equation is printed in the output file.

**FUNC** plot a known function. The function is defined in the routine VPOT. To plot the function  $y=5*(1-\cos(x))$ , the following Fortran statements would be used:

```
FUNCTION VPOT(X)
  VPOT=5.0*(1.0-COS(X))
  RETURN
END
```

VPOT must be a function of only x.

**ULEAST** fit the data to user supplied basis functions.



The basis functions are defined in the Fortran function BASIS. BASIS is a function of an integer identifying the basis function and x. The program accepts a maximum of ten basis functions. The basis function coefficients are printed in the output file. The following Fortran statements define a polynomial set of basis functions:

```

FUNCTION BASIS(I,X)
  BASIS=X**I
  RETURN
END

```

DTITLE is an arbitrary character string used to identify the curve on the plot.

**CARD EIGHT:** The structure of card eight depends on which plot option was selected on card seven.

**MARK:** IMARK (format I1)

IMARK determines the type of mark to be plotted at each data point. The default mark is a plus sign (+). The possible marks are:



- 1 = dot ( . )
- 2 = plus sign ( + )
- 3 = asterick ( \* )
- 4 = Capital letter O
- 5 = Capital letter X

The mark is currently plotted only in the default color.  
DTITLE is not sent to the plotter for IMARK.

**SPLINE,LEAST,FUNC OR ULEAST:** IPEN, ICOLOR,  
INTENS, LSTYLE, LWIDTH (format 5I5)

IPEN selects the pen color for paper type plots. The default color is black. The possible colors for the UT Zeta plotters are:

- 1 = black
- 2 = red
- 3 = green
- 4 = blue

ICOLOR selects the color for color monitors. The possible colors are:



- 0 = normal device color
- 1 = red
- 2 = green
- 3 = yellow
- 4 = blue
- 5 = magenta
- 6 = cyan
- 7 = white
- 8 = black
- 9 = complement of normal device color

INTENS sets the line intensity on a terminal and ranges from 0 to 32000. INTENS has not been tested during program development and the DI-3000 documentation is vague, so I cannot make any recommendations regarding its use.

LSTYLE sets the style of the line and ranges from 0 to 32000. LSTYLE changes a solid line into a dashed or dotted line. LSTYLE = 0 gives a solid line.

$0 < \text{LSTYLE} < 11$  gives a dotted line determined by the plotting device being used.  $\text{LSTYLE} > 10$  gives DI3000



produced line styles. LSTYLE = 1 or 2 gives nice looking results.

LWIDTH sets the width of a line and ranges from 0 to 32000. LWIDTH has not been tested during program development.

**ULEAST:** IBASIS (format I2)

IBASIS is the number of basis functions defined in the function BASIS. IBASIS must be greater than 0 and less than 11.

The following two cards are used to add text to the plot. They may be repeated any number of times.

**CARD NINE:** TEXT format(A40)

TEXT is an arbitrary DI-3000 text string up to 40 characters long. The string must be input with delimiters.

**CARD TEN:** XNOTE, YNOTE, TXTHGT, TXTANG

XNOTE, YNOTE, TXTHGT are defined as in Card 4.

TXTANG is the angle the text makes with the bottom of the paper. If TXTANG = 0, the string is parrallel to the bottom of the paper. The angle of rotation is counter-clockwise, i.e. If TXTANG = 90, the text is parallel to the edge of the paper and



reads from bottom to top.

**OUTPUT:** The program sends an output file and a metafile to the VAX. The output listing echoes an ordered list of the input data points, the 300 cubic spline points used to interpolate the data and the results of any least squares fitting. The program reports  $n$  weighted standard deviations for the least squares fitting procedure.

**TRANSLATING THE METAFILE:** The metafile is translated on the VAX 8600 using the command METATRANS. Metafiles produced on the CRAY must be translated on the VAX 8600 because the metafiles are not compatible with the AGL, CDC or NGP metatranslator. After entering the METATRANS command, the following screen is encountered:



---

\*\*\*\*\*

## DI-3000 METAFILE TRANSLATOR

\*\*\*\*\*

### Devices Drivers:

| Code | Description                          |
|------|--------------------------------------|
| ---- | -----                                |
| GIG  | DEC Gigi                             |
| PTX  | Printronix plotter                   |
| T10  | Tektronix 4010                       |
| 405  | Tektronix 4105                       |
| 407  | Tektronix 4107/4109                  |
| 415  | Tektronix 4115                       |
| TL8  | Talaris 800/1200/2400                |
| ZTA  | Nicolet Zeta plotters                |
| RJZ  | UT Austin Comp. Center Zeta plotters |
| EXIT | Exit metafile translator             |
| QUIT | Quit metafile translator             |

Enter the Device Driver code:

---

Make the appropriate selection and wait for a few seconds while the machine whirs. The metatranslator prompt is "M>". The following are a few of the more commonly used commands. For more detailed information refer to the DI-3000 Metatranslator Users Manual.



SET METAFILE N - N is a number, between 1 and 5, that identifies the metafile to the translator.

SET VIEWPORT (XMIN XMAX YMIN YMAX) - This command changes the extent of the plotting surface covered by the plot. By default the entire surface is covered, this is equivalent to the command SET VIEWPORT (-1. 1. -1. 1.). The absolute values of the maximum and minimum numbers must be less than 1. This command can only shrink the plot.

DRAW PICTURE I METAFILE J - Draw picture I from metafile j. I is equal to 1 in all cases for the FUNPLOT program.

QUIT - We are all done plotting, send the device commands to a disk file.

The metatranslator automatically sends the plotting commands for hardcopy devices to disk. UT zeta plot files are sent to the file ZETA07.PLT. Postscript files, Apple Laserwriter files, are sent to the file POSTS.DAT.

The following input deck generates Figure 3-24. Some of the input lines do not conform to the required format specification.

JOB,JN=Q2824TH,T=25.

ACCOUNT,US=,UPW=.

ACCESS,DN=FUNPLOT,PDN=FUNPLOT,OWN=CMAO273.

FETCH,DN=BASIS,TEXT='COS24TH.FOR'.

ASSIGN,DN=\$IN,A=FT05.



ASSIGN,DN=\$OUT,A=FT06.

LIB,DN=DI3LIB:GRAFLIB.

LIB,DN=IMSLIB.

CFT,I=FUNPLOT,L=0.

CFT,I=BASIS.

LDR,LIB=DI3LIB:GRAFLIB:IMSLIB.

ACCESS,DN=METAPLT.

DISPOSE,DN=METAPLT,TEXT='Q2824TH.MFL'.

/EOF

11

0.00            0.00

-22.65           2.270

25.0            2.624

40.25           5.613

62.85           9.531

91.6            11.337

113.65           9.965

142.95           3.947

157.7           2.155

180.0           0.0

205.0           2.624

\$Q28 COS(2\*THETA)+COS(4\*THETA)\$            500.0    940.0    25.0

\$Q28\$                    -30.0    210.0    TIC    25.0



```

0.00   180.0   45.0       1  2  5$(F5.1)$
$V(KCAL/MOLE)$           -1.0   12.0   TIC
0.0    12.0    2.0       1  1  6$(F4.1,2X)$
3      700.0   700.0   15.0
MARK $$
2
SPLINE$SPLINE$
  1
ULEAST$COS(2X)+COS(4X)$
  3      3
.
2
$FIGURE 3-24$
500.0 975.0 30.0 0.0
$+ Data Points$
800.0 680.0 15.0 0.0

```



## Bibliography

1. P. Pulay in "Modern Theoretical Chemistry vol. 4: Applications of Electronic Structure Theory", ed. H. F. Schaefer, Plenum Press, 1977.
2. M. Dupis, J. Rys and H. F. King, J. Chem. Phys., 111 (65) 1976.
3. P. Pulay, Chem. Phys. Lett., 393 (73) 1980.
4. J. A. Pople, R. Krishnan, H. B. Schlegel and J. S. Binkley, Int. J. Quant. Chem. Symp. 225 (13) 1979.
5. W. J. Hehre, L. Radom, P. v. R. Schleyer and J. A. Pople, "Ab Initio Molecular Orbital Theory", John Wiley and Sons, 1986.
6. P. Pulay, G. Fogarasi, F. Pang and J. E. Boggs, J. Am. Chem. Soc. 2550 (101) 1979.
7. J. E. Boggs and F. R. Cordell, J. Mol. Struct. (Theochem) 329 (78) 1981.
8. L. Schafer and coworkers in a series of papers titled "Ab Initio Studies of Structural Features not Easily Amenable to Experiment" appearing in J. Mol. Struct. A summary of his early results using the 4-21 basis set may be found in J. Mol. Struct.(Theochem) 349 (86) 1982.
9. J. E. Boggs, J. Mol. Struct. 1 (97) 1983.
10. A. H. Lowrey and R. Gilardi private communication.
11. P. Pulay, Theoret. Chim. Acta. 299 (50) 1979.
12. J. E. Boggs and Z. Niu, J. Comp. Chem 46 (6) 1985.
13. W. J. Hehre, R. Ditchfield and J. A. Pople, J. Chem. Phys. 2257 (56) 1972.



14. J. E. Boggs, M. Altman, F. R. Cordell and Y. Dai, *J. Mol. Struct.* 373 (94) 1983.
15. G. Pfafferott, H. Oberhammer, J. E. Boggs and W. Caminati, *J. Amer. Chem. Soc.* 2305 (107) 1985.
16. C. Chabalowski, P. C. Hariharan and J. J. Kaufman, *Int. J. Quant. Chem. Symp.*, 643 (17) 1983.
17. J. J. Kaufman, P. C. Hariharan, C. Chabalowski and M. Hotokka, *Int. J. Quant. Chem. Symp.*, 221 (19) 1986.
18. J. J. Kaufman, *Int. J. Quant. Chem.*, 179 (29) 1987.
19. D. S. Marynick, A. K. Ray and J. L. Fry, *Chem. Phys. Lett.*, 429 (116) 1985.
20. S. D. Kahn, W. J. Hehre and J. A. Pople, in press.
21. Gaussian 82, J. S. Binkley, M. J. Frisch, D. J. De Frees, K. Ragavachari, R. A. Whiteside, H. B. Schlegel, E. M. Fluder and J. A. Pople, Department of Chemistry, Carnegie-Mellon University, Pittsburgh, Pennsylvania.
22. K. D. Dobbs, unpublished work.
23. P. G. Jasien, W. J. Stevens and M. Krauss, *J. Mole.Struct. (Theochem)*, 197 (139) 1986.
24. R. Krishnan, J. S. Binkley, R. Seeger and J. A. Pople, *J. Chem. Phys.* 650 (72) 1980.
25. Z. Niu and J. E. Boggs, *J. Mol. Struct. (Theochem)* 381 (109) 1984.
26. GRAFMAKER, Precision Visuals, Inc. Boulder, CO, 1984.



27. R. Stolevik and P. Rademacher, *Acta Chem. Scand.* 672 (23) 1969.
28. M. Rey-Lafon, *J. Chem. Phys.* 5324 (71) 1979.
29. B. Krebbs, J. Mandt, R. E. Cobbledick and R. W. H. Small, *Acta Cryst.* 402 (B35) 1979.
30. A. Filhol, G. Bravic, M. Rey-Lafon and M. Thomas, *Acta Cryst.* 575 (B36) 1980.
31. B. J. Duke, *J. Mol. Struct.* 109 (50) 1978.
32. K. I. Rezchikova and V. A. Shlyapochnikov, *Izv. Akad. Nauk SSSR, Ser. Khim.*, 947 (4) 1985.
33. F. R. Cordell, work in progress.
34. S. F. Boys, in P. O. Lowdin (Ed.), *Quantum Theory of Atoms, Molecules and the Solid State*, Academic Press, New York 1968 p. 253.
35. R. S. Mulliken, *J. Chem. Phys.* 1833 (23) 1955.
36. P. Pulay, G. Fogarasi, G. Pongor, J. E. Boggs and A. Vargha, *J. Am. Chem. Soc.* 7037 (105) 1983.
37. J. N. Macdonald, private communication.



## VITA

Floyd Richard Cordell was born Floyd Richard Bull in Wiesbaden, West Germany on December 5, 1958. His biological father died in 1959. His mother, Roberta Diane Adams, married Glenn Alwin Cordell May 2, 1964. Now an Army Brat, he attended several different schools before graduating from Mary Carroll High School, Corpus Christi, Texas in 1976. He entered the University of Texas at Austin in August, 1976. He graduated with Special Honors on August 22, 1980 and received the degree of Bachelor of Science. On the same day, he was commissioned an Ensign in the United States Navy.

Ensign Cordell reported to Naval Aviation Schools Command for training as a Naval Flight Officer in October, 1980. He graduated at the top of his class from both VT-10 and VT-86 and received his "Wings" September 30, 1981.

Ensign Cordell reported to Attack Squadron 128 in December 1981 for training as an A-6 Bombardier/Navigator. After completing the syllabus, he reported to Attack Squadron 196 in October 1982. LT(j.g.) Cordell recieved the 1983 "Student B/N of the Year" while deployed aboard USS Coral Sea.

While assigned to VA-196, LT Cordell completed an Around the World Cruise onboard USS Coral Sea, an Indian Ocean Cruise onboard USS Constellation and accumulated over 1100 flight-hours



and 300 carrier landings in the A6 Intruder.

In August 1985, LT Cordell was ordered to the University of Texas at Austin and entered The Graduate School. After completing his Master of Arts degree, LT Cordell will report to Attack Squadron 128 for refresher training in the A6 Intruder and will subsequently be assigned to the Navy's newest Medium Attack Squadron, VA-155.

Floyd Cordell married Sandra Lou Blalock on March 17, 1978. They have two children, Rebecca, born October 20, 1981 and Elizabeth, born October 4, 1983.

Permanent address:       5037 Cascade Drive  
Corpus Christi, Texas











Thesis  
C754628 Cordell  
c.1 An AB initio study of  
dimethyl nitramine.

Thesis  
C754628 Cordell  
c.1 An AB initio study of  
dimethyl nitramine.

thesC754628

An AB initio study of dimethyl nitramine.



3 2768 000 72897 6

DUDLEY KNOX LIBRARY